AD-A111 774 NIELSEN ENGINEERING AND RESEARCH INC MOUNTAIN VIEW CA F/G 20/4
STUDY OF FLOW FIELDS AND STORE FORCES IN CLOSE PROXIMITY TO A T--ETC(U)
MAY 81 F K GOODWIN, J N NIELSEN

UNCLASSIFIED NL

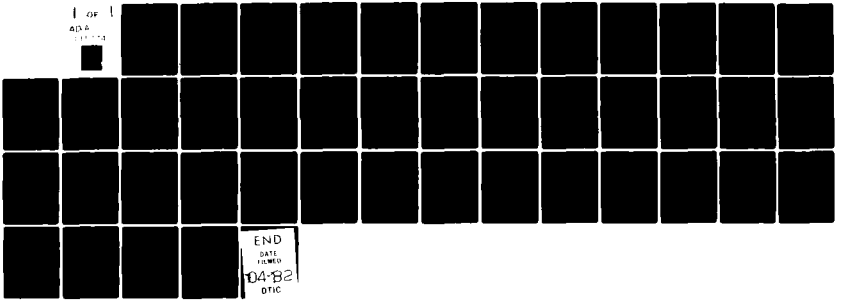

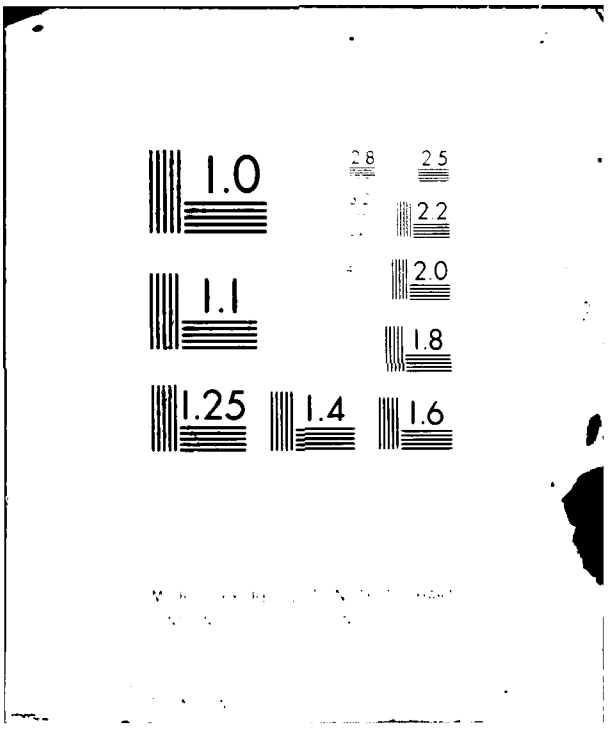
1.0
2.8
2.5
2.2
2.0
1.1
1.8
1.25
1.4
1.6

STUDY OF FLOW FIELDS AND STORE FORCES IN CLOSE PROXIMITY TO A TRIPLE EJECTION RACK AT TRANSONIC SPEEDS

Frederick K. Goodwin and Jack N. Nielsen
Nielsen Engineering & Research, Inc., Mountain View, California

14 pp only pl

ABSTRACT

The information presented in this paper shows what parent aircraft effects are important when determining the forces and moments acting on a store in close proximity to a triple ejection rack. The large gradients in the store forces and moments which exist near the carriage position are demonstrated. Areas are shown in which improvements to the AFFDL/Nielsen subsonic store separation computer program are required if the launch dynamics of a store released from such a configuration are to be accurately predicted.

INTRODUCTION

Recently the AFFDL/Nielsen subsonic store separation program[1] has been used to make predictions for comparisons with flight and wind-tunnel captive store loads on a MK-83 bomb on an F-4C aircraft. The bomb was mounted on the bottom station of a triple ejection rack (TER) with dummy bombs mounted on the two shoulder stations. The comparisons are presented in Reference 2 and indicate that deficiencies may exist in the TER model in the computer program. The work of Maddox, Dix, and Mattasits[2] describes a carefully monitored flight test program designed to provide data to compare with wind-tunnel data and mathematical predictions.

The work described in this paper had two main objectives. The first was to provide a data base which could be used to determine where deficiencies in the computer program exist. The second objective was to attempt to identify the deficiencies by making comparisons of computer program results with the data.

The test program was conducted in the 4-Foot Transonic Wind Tunnel (4T) of the Propulsion Wind Tunnel Facility (PWT) at the Arnold Engineering Development Center (AEDC). The test program was jointly sponsored by the Naval Weapons Center (NWC) and the Air Force Wright Aeronautical Laboratories (AFWAL/FIGC).

This paper will briefly describe the test program and the types of data obtained. A discussion of the experimental results follows this. The compatibility of the captive or attached loads with the grid loads is discussed. Then phenomena exhibited by the data during the parent aircraft build-up sequence are discussed. Finally, the paper presents some comparisons between the experimental data and predictions made using the computer program of Reference 1. The test program and the experimental results are discussed in

more detail in Reference 3, the final technical report on this investigation. That report also contains more comparisons between data and predictions.

This work was supported by the Naval Weapons Center, China Lake, California, under Contract N60530-79-C-0169. The Technical Coordinator was Mr. Ray E. Smith.

NOMENCLATURE

CA	axial-force coefficient, axial force/qS
CLL	rolling-moment coefficient, rolling moment/qSD
CLM	pitching-moment coefficient, pitching moment/qSD
CLN	yawing-moment coefficient, yawing moment/qSD
CN	normal-force coefficient, normal force/qS
CY	side-force coefficient, side force/qS
D	store maximum diameter, 0.7 inch
M_∞	free-stream Mach number
q	free-stream dynamic pressure
S	store frontal area, 0.385 in^2
VY/V	local sidewash velocity divided by free-stream velocity, positive to the right when viewed from the rear
VZ/V	local upwash velocity divided by free-stream velocity, positive up when viewed from the rear
X_p	distance from tip of store nose, negative aft
Z_p, Z_s	vertical distance measured from carriage position on rack, positive down
α_s	store angle of attack relative to free stream

WIND-TUNNEL TEST PROGRAM

The purpose of the test program was to provid a systematic set of data which could be used in evaluating and improving the capability of the computer program of Reference 1 to predict the aerodynamic forces and moments acting on stores carried in a TER configuration. The capability of calculating store forces and moments with the store in the carriage position is of interest as well as the capability in the detached position. For this reason force and moment tests were performed using both bracket supported and captive trajectory system (CTS) supported force models. In order to calculate analytically the forces and moments acting on a store, the aircraft induced flow field in which the store is immersed must be predicted. Flow-field survey data were taken, using a 20° half angle conical probe, to provide information on the aircraft induced flow field.

The basic details of the five-percent (1/20th) scale model of the F-4C used in the tests are shown in Figure 1. The model is geometrically similar to the full-scale aircraft except that the part aft of the engine exhausts has been removed to minimize CTS interference. This removal does not influence the results of this test program.

Details of the F-4C pylons are shown in Figure 2. For most tests only the left-wing inboard pylon was used. All testing was done under the left wing. Pylons were not installed on the right wing for any of the tests.

The triple ejector rack (TER) used in the test program is shown in Figure 3. The TER was used in conjunction with the left-wing inboard pylon. This rack model simulates sway braces and ventilating passages.

The stores which were used are shown in Figure 4. They are models of the MK-83 bomb. Figure 4(a) shows the actual bomb shape and Figure 4(b) shows a model which was modified for CTS sting support. Models with identical body shapes but without tail fins were also used. The dummy stores used on the shoulder locations of the TER were the shape shown in Figure 4(a). Both finned and unfinned models were used. Four force models were used during the captive force and moment tests. Tests were performed with both configurations shown in Figure 4 with and without tail fins.

The Mach number range used in the test program was 0.6 to 0.95. All testing was performed at a nominal Reynolds number per foot of 3.5×10^6. The store angle of attack was varied from -4° to 16°. Since the store is oriented on the TER one degree nose down relative to the aircraft reference waterline (aircraft angle of attack is measured relative to this line), the aircraft angle of attack varied from -3° to 17°.

Eight parent aircraft configurations were used during the test program. They are listed in Table 1. The first column lists the eight numbers. These numbers will be used in the next sections of this paper. The remaining eight columns list model components which could be attached to the parent F-4C. These components are:

$P_{\mathbb{C}_L}$	fuselage centerline pylon
P_I	left-wing inboard pylon
P_O	left-wing outboard pylon
T	TER attached to left-wing inboard pylon
$(S_2)_U$	unfinned dummy store attached to outboard shoulder station on TER
$(S_3)_U$	unfinned dummy store attached to inboard shoulder station on TER
$(S_2)_F$	finned dummy store attached to outboard shoulder station on TER with fins vertical and horizontal
$(S_3)_F$	finned dummy store attached to inboard shoulder station on TER with fins vertical and horizontal

Further details of the test program including lists of the specific runs made are contained in Reference 3.

RELATIONSHIP BETWEEN ATTACHED AND GRID LOADS

A significant problem in store loads is whether a sting-supported store will yield the attached store loads (forces and moments) as it approaches the attached-store position as close as possible under practical testing conditions without making contact with the rack. In fact, the nature of the interference forces on the store for small gaps between store and rack is not well understood.

Knowledge of the loads on a store in close proximity to the attached position is not extensive, but light has been shed on this subject by the tests of Dix[4]. The tests were of MK-83 bombs on a TER rack mounted on a model of an F-4C airplane and included both attached loads and loads on a sting-supported bomb. His results are presented for $\alpha_s = 0°$ and do not include parent aircraft component build-up results. His data show that the captive loads cannot be obtained by extrapolating CTS data to zero Z/D in general. For some coefficients (CLM, CA, CLN), such extrapolation was better than for others (CN, CY). Large changes occurred for $Z/D < 0.2$ which could not be measured with the CTS system because of limitation in accuracy of positioning the store.

In this investigation a more extensive investigation was made of the problem, and the effects of angle of attack and configuration build-up were measured. Also flow-field data in the vicinity of the attached bottom store position were taken.

Stores S_{MF}, Figure 4(b), and S_{MU}, an unfinned version of this store are the ones tested both on the attached-loads balance and the CTS sting supported balance. Data for store S_{MF} in combination with configuration 3 of Table 1 (F-4C, inboard pylon, TER) are shown in Figure 5. In Figure 5(a) the normal-force coefficient is shown versus Z_P/D for five angles of attack at $M_\infty = 0.6$. The sting data extend down to $Z_P/D = .07$. There is a large change in CN in the range $0 < Z_P/D < .07$ as indicated by the attached-store data which cannot be reproduced by extrapolating the sting results to zero gap. This range of Z_P/D representing only 0.05 in. model scale, 1.0 in full scale, produces surprisingly large interference forces which increase with angle of attack.

Examination of the other parts of Figure 5 for the other coefficients shows that extrapolation of the sting data to $Z_P = 0$ is fairly accurate. The question naturally arises whether the attached loads are accurately measured. It is our belief based on the overall consistency of the data as well as the results of Dix that the attached loads are valid.

These results are typical of those obtained for store S_{MU} and for other parent aircraft configurations.

EFFECT OF CONFIGURATION ON ATTACHED LOADS

Attached store loads (forces and moments) were measured for configurations 3, 4, 5, 6, and 8 of Table 1. The variations of loads for store S_{AF}, Figure 4(a), at $M_\infty = 0.6$ with angle of attack are shown in Figure 6 for the above five configurations. Figure 6(a) shows that at angles of attack between -4° and +8°, configuration 3 yields the least normal force (positive upward). Configurations 4 and 8, which only have one shoulder store, yield more normal force; and configurations 5 and 6, with two shoulder stores, yield the largest normal forces. What is of particular interest is that the addition of fins to the shoulder stores (4 vs 8 and 5 vs 6) has a small effect on normal force. Also at angles of attack above 8°, the effects of configuration differences are much less than at lower angles of attack.

The side-force variation with α_s shown in Figure 6(b) shows that the side force is relatively insensitive to configuration especially for angles of attack less than 8°. Positive side force is directed towards the fuselage from the left-wing inboard pylon.

Pitching-moment coefficients shown in Figure 6(c) are generally nose down. For angles of attack less than about 6°, the effect of configuration on the magnitude of the pitching-moment coefficient is similar to its effect on normal force. However in the range above 6° to 8°, configurations 5 and 6 have smaller pitching moments than configurations 4 and 8. Again adding fins to the shoulder stores causes negligible effect.

The yawing-moment coefficients in Figure 6(d) are slightly nonlinear with α_s from -4° to 16° and are positive. There are significant differences due to configuration changes, but the addition of fins to the shoulder store has a negligible effect.

The rolling-moment coefficients in Figure 6(e) are positive, nonlinear, and have maxima around 6° to 8°. The configuration effects are significant. The addition of the fins to the shoulder stores causes a significant effect in the higher angle range.

The same kind of data as Figure 6 for other Mach numbers show the same general qualitative effects.

EFFECT OF CONFIGURATION ON GRID LOADS

The grid loads on the bottom store as it moves downward from close proximity to the rack are influenced by angle of attack, configuration, Mach number, addition of fins to the shoulder stores, and the number of shoulder stores. Figure 7 shows the loads on store S_{MF} at $M_\infty = 0.6$ as influenced by configuration and store vertical position. Only the first 1.25 diameter of store vertical position are shown.

Examination of the normal-force results shows the least normal force for configuration 2 with a small positive increment due to addition of the TER. Addition of one shoulder store contributes positive increments about twice those due to the TER. Addition of the other shoulder store adds an even larger positive increment to the normal force. Addition of the fins to the shoulder stores adds further small positive increments in normal force. It is concluded that the addition of the shoulder stores are most important, followed by the addition of the TER, and finally the addition of the fins to the shoulder stores.

The side-force results in Figure 7(b) show that the largest effects of configuration occur at small Z_P/D. The effect of adding the second shoulder store is to almost cancel the increment due to adding the first. The effect of adding fins to the shoulder stores is again fairly small.

The pitching-moment results show the same qualitative effects as the normal-force results. The yawing-moment results show large configuration effects at small Z_P/D (on an expanded scale) and small effects at large Z_P/D. The store alone has a rolling-moment coefficient of .037 at $\alpha_s = 0°$ because of fin cant. Additional rolling moments of about the same magnitude can be developed at small Z_P/D because of configurational differences. At these small values of Z_P/D, increments in CLL as large as 0.01 can be developed by the addition of fins to the shoulder stores.

COMPARISON BETWEEN EXPERIMENT AND THEORY

The basic objective of the experimental investigation was to provide data for validating the computer program of Reference 1 and to provide insight into methods for upgrading the computer program. Accordingly the comparisons between theory and experiment are directed toward these ends. In order to make sure comparisons meaningful, it is of interest to describe the main assumptions that are made in the computer program especially with respect to pylon, rack, and stores and to suggest areas where refinements in the computer program may appear necessary.

The computer program for calculating the parent aircraft flow field is based on linear theory, Laplace's equation for the flow field with the Glauert-Prandtl theory to account for compressibility. The fuselage, which can be non-circular, is modeled by using sources, doublets, and high-order solutions along the axis of the fuselage to satisfy its boundary conditions, with a vortex-lattice layout on the wing to satisfy the wing boundary conditions. The vortex-lattice system is imaged in the fuselage (assumed circular). Wing thickness is modeled by source panels. Account is taken of airflow through inlets and ducts by changing the effective cross-sectional area distribution of the body.

The pylon is modeled with regard to thickness by source panels and with regard to the normal velocity boundary condition by a vortex-lattice layout.

The rack is modeled for volume by a body of revolution.

The stores are modeled for volume by three-dimensional source distributions along their axes. No mutual interference between stores or between stores and rack is accounted for. No doublets to model store angle of attack distributions are included. The tail fins of the shoulder stores are not modeled.

The forces and moments acting on the ejected store are calculated by slender-body theory. Both upwash and sidewash distributions are taken into account. Also a loading due to buoyancy is included in the calculation. If the flow separates at some axial station, crossflow drag theory is used to calculate the loading downstream of separation. The tail fin contributions are determined using the spanwise variation of induced downwash across the tail span together with reverse-flow theorems in a method which has accuracy nearly equivalent to full linear theory.

In the ensuing comparisons, the effects of adding the pylon to the clean airplane, the effect of adding the rack to the pylon, and the effect of adding the shoulder stores to the rack will be isolated and compared with theory. These increments are all to be added to the clean airplane characteristics as a base configuration. It is therefore of interest to examine the comparison between experiment and theory for the clean airplane.

In Figure 8 the downwash and sidewash angles are shown along the $Zp/D = 0$ location for $M_\infty = 0.6$ for various angles of attack. The store nose location is $Xp = 0$. It is noted that the experimental upwash angle is predicted fairly well up to about 8° angle of attack although it is consistently less than theory. Significantly large deviations between experiment and theory occur by the time $\alpha_s = 16°$ is reached. The sidewash is predicted well up to $\alpha_s = 8°$.

In Figure 9, the loads on store S_{MF} in combination with the clean airplane at $Z_p/D = 0$ are shown for the angle of attack range from 0° to 16° and compared with the predictions of the computer program. The normal force is predicted well up to about 8°, and is about half of its free-stream value for the same angle of attack. The side force is predicted well up to about 12°. The pitching moments and yawing moments are not well predicted, but they are generally less than those for the store in the free stream. The center-of-pressure position for yawing moment is in error by as much as 0.5 diameters. In the theory, the separation position on the boattail corresponding to α_s has been used. The results of Figure 8 show that the average angle of attack on the boattail is much less than α_s. Accordingly separation occurs more aft than predicted. This yields more download on the boattail and more nose-up moment.

The effects on the flow field of adding the pylon to the airplane can be determined by subtracting data for configuration 1 from that for configuration 2. In this way the effects of the pylon can be examined unmasked by configuration 1 effects. The next two figures show the pylon effects on upwash and sidewash at $M_\infty = 0.6$ for the following conditions:

Figure	α_s	Z_p/D
10	0	0
11	4°	0

It is clear that the pylon effect on the flow field is small and accurately predicted for the conditions shown.

It would be normally assumed that if the flow angles induced by the pylon at the store location are small, that the corresponding loads induced by the pylon on the store would be small. As an example, consider Table 2 which shows the loads on the S_{MF} store for four cases due to the addition of the pylon. Generally speaking the difference between experiment and theory is not large so that the loads were satisfactorily predicted.

The effects on the flow field of adding the rack to the airplane pylon combination are shown in Figures 12 and 13. These results for both data and theory represent configuration 3 minus configuration 2. The first thing that is clear is that the induced angles of upwash and sidewash are generally several times larger than those due to the pylon at $Z_p/D = 0$. It is also apparent that the effect of the rack attenuates much in going from $Z_p/D = 0$ to $Z_p/D = 1.0$. For instance, the induced upwash maxima fall from about -0.04 to about -0.01 in this distance. It happens that the $Z_p/D = 0$ position is about one diameter below the centerline of the rack and the $Z_p/D = 1.0$ position is about two diameters below the rack centerline. This suggests that the upwash is strongly source dominated. The effect of the rack is modeled solely by sources in the theory. However, the theoretical source effect is too weak, particularly at $Z_p/D = 0$.

Looking at the sidewash angle, the maximum sidewash exists at $Z_p/D = 0$ and attenuates greatly at $Z_p/D = 1$. The theory predicts no sidewash since the rack sources produce none directly below themselves. It is clear that

mechanisms to produce sidewash due to addition of the rack must be introduced into the computer program.

It is not to be expected that the loads on store S_{MF} due to addition of the rack to the pylon will be predicted well for $Z_p/D = 0$ since the upwash and sidewash are significant at this location, and the theory underpredicts them. It is of interest to examine the load increments due to the rack in a similar form to that for the pylons.

Examination of Table 3 immediately shows that the computer program gives no contribution to CY, CLN, and CLL due to addition of the rack. This shortcoming of the method is more important at $\alpha_s = 4°$ than $\alpha_s = 0°$ since the sidewash is greater at $\alpha_s = 4°$. An error of about 0.2 in side-force coefficient occurs and about 0.045 in yawing-moment coefficient. There is a surprising effect on rolling-moment at $\alpha_s = 4°$ and $Z_p/D = 0$, the value of CLL for configuration 3 being 0.064 and for configuration 2 being 0.025. There is a sidewash gradient between the top and bottom fins of the X arrangement which is, if anything, weaker at $Z_p/D = 0$ than at $Z_p/D = 1.0$. Since the effect does not occur at $Z_p/D = 1.0$, some other phenomenon must be producing this difference which is equivalent to about 2° of cant of all fins. The phenomenon is believed due to a trailing vortex from the rack pylon.

The effect of adding the shoulder stores will be determined by taking the difference between the results for configuration 5 and configuration 3. Any effects of the fins of the shoulder stores will not be included by this means. Also, the theory does not include the effect of shoulder store fins, and these have been shown to be small.

Figures 14 and 15 show the effects on the upwash and sidewash angles along the store axis position for $\alpha_s = 0°$ and two vertical positions at $M_\infty = 0.6$. Both experiment and theory are shown. The upwash angles get to be nearly as large as -5°, while the sidewash is generally much less than 1°. The theory in some cases predicts the upwash well, but more often underpredicts it. The degree of agreement is surprising in view of the fact that only the volume effect of the two stores are modeled with no interference between them. Thus the theoretical VZ/V increment due to the shoulder stores at a fixed value of Z_p/D does not vary with α_s. The theoretical sidewash increment, VY/V, is small.

At $Z_p/D = 0$ some sidewash exists but at $Z_p/D = 1$ it is negligible for $\alpha_s = 0°$. The rapid decay of this sidewash suggests that some dipole distribution is causing it. The two shoulder stores are subject to sidewashes which are not equal. Dipoles to cancel these sidewash boundary conditions will produce differential sidewash under the rack. This represents a possible source of the sidewash. Likewise doublets to cancel the downwash distribution along the shoulder stores would modify the upwash and could account in part for the differences between experiment and theory. Some account of mutual interference between shoulder stores and rack-pylon may be required to get accurate flow fields. The shoulder stores can change the rack-pylon lifting surface boundary condition, the pylon can influence the boundary conditions of the shoulder stores, and the shoulder stores can interfere with each other. These interferences can be evaluated to see which are of sufficient magnitude to influence the flow field.

It is of interest to see the magnitude of the loads on the bottom store induced by the shoulder stores. Table 4 presents the results for two angles of attack and two vertical positions. The table shows that the addition of shoulder stores has its maximum effects on CN and CLM, and has generally small effects on CY, CLN, and CLL. This result is in general accordance with the flow-field comparisons. It is noted that the changes in CN and CLM are better predicted at $Z_p/D = 1.0$ than at $Z_p/D = 0$, a fact also in agreement with the flow-field results. Some error at $Z_p/D = 0$ is due to prediction of the flow field. But even with an accurate flow-field prediction, some errors in loads will be predicted at this position. It is probable that mutual interference between all three stores, at least for volume effects, will influence the loads.

CONCLUSIONS

ATTACHED VERSUS GRID LOADS

1. The forces and moments on a store in close proximity to a TER can exhibit large changes within the first few tenths of a store diameter from the attached position.

2. It is not generally feasible using present measuring methods to extrapolate loads measured on a CTS supported model to those for the attached position.

ATTACHED LOADS

1. Adding the shoulder stores to the rack had the following effects on the attached loads of store S_{AF} at $M_\infty = 0.6$.

   (a) The normal forces received a large positive increment due to addition to the rack of the outboard shoulder store in the low angle of attack range, and further increments of comparable magnitude by subsequent addition of inboard shoulder store. At high angles of attack, $\alpha_s > 10^c$, the increments became much smaller.

   (b) The changes in side-force coefficient were small.

   (c) There were definite changes in the pitching-moment coefficient, but these were greater than those in yawing-moment coefficient.

   (d) Rolling-moment coefficient exhibited significant changes.

2. Adding fins to the shoulder stores under the conditions of (1) generally causes small changes in the store loads except at large angles of attack.

GRID LOADS

1. At $M_\infty = 0.6$ and at $\alpha_s = 0°$ with store S_{MF} within 1 store diameter of the rack the most important things influencing the bottom store loads are in

decreasing order of importance:

(a) Addition of shoulder stores to TER.
(b) Addition of TER to pylon.
(c) Addition of fins to the shoulder stores.

Changing the angle of attack to 8° does not change the foregoing conclusion.

2. The addition of fins to the shoulder stores for the ranges of M_∞ and α_s of the tests has a generally small effect, and the effect is largest at small values of Z_p/D.

COMPARISON BETWEEN EXPERIMENT AND THEORY

1. For the clean airplane, the upwash and sidewash angles near the store location at the inboard pylon are predicted adequately for preliminary design purposes to $\alpha_s = 8°$ but not up to $\alpha_s = 16°$.

2. For store S_{MF} in combination with the clean airplane near the attached inboard position, the normal force, side force, and rolling moment are well predicted by the computer program up to $\alpha_s = 8°$. However, the pitching moment and yawing moment are not predicted well probably as a result of movement of the separation position on the boattail afterbody due to the nonuniform flow field and its resulting effects on afterbody and tail normal forces.

3. Adding the pylon to the clean airplane produced downwash and sidewash changes near the location of the attached store on the inboard pylon which were usually less than 0.5° and which were accurately predicted by the computer program.

4. The loads on store S_{MF} at $Z_p/D = 0$ and 1 due to the addition of the pylon were predicted satisfactorily. In magnitude they correspond in some cases to a change in angle of attack of the store in the free stream of 1° to 2°.

5. Adding the TER to the airplane-pylon combination caused changes in downwash angle and sidewash angle at the attached store position. They are several times greater than those due to the addition of the pylon, and the theory generally underpredicts these changes. In fact the theory predicts no sidewash changes since the rack is modeled by a body of revolutions with volume only (sources and sinks).

6. Generally the computer program predicts zero yawing-moment, side-force, and rolling-moment contributions due to addition of the rack since no sidewash is predicted. The normal-force and pitching-moment increments are fairly well predicted.

7. The upwash distribution due to adding the shoulder stores to the rack is predicted fairly well at $Z_p/D = 1.0$ but is underestimated at $Z_p/D = 0$. The use of doublets to cancel the upwash acting on the shoulder stores could be one source of upwash not included in the theory. Another source could be mutual interference between shoulder stores and rack pylon.

REFERENCES

1. Goodwin, F. K. and Dillenius, M. F. E.: Extension of the Method for Predicting Six-Degree-of-Freedom Store Separation Trajectories at Speeds Up to the Critical Speed to Include a Fuselage with Noncircular Cross Section. Vol. II - Users Manual for the Computer Program. AFFDL-TR-74-130, Vol. II, November 1974.

2. Maddox, A. R., Dix, R. E. and Mattasits, G. R.: In-Flight Measurements of Captive Loads on a Store as Compared with Wind Tunnel and Mathematical Simulation. NWC TP 6026, April 1978.

3. Goodwin, F. K. and Nielsen, J. N.: Experimental and Theoretical Study of Flow Fields and Store Forces in Close Proximity to a Triple Ejection Rack at Transonic Speeds. NWC TP 6210, June 1980.

4. Dix, R. E.: Comparison of Two Methods Used to Measure Aerodynamic Loads Acting on Captive Store Models in Wind-Tunnel Tests. AEDC-TR-76-122, September 1976.

Table 1. Parent Aircraft Configurations.

CONFIG. NO.*	P_{ℓ}	P_I	P_O	T	$(S_2)_U$	$(S_3)_U$	$(S_2)_F$	$(S_3)_F$
1								
2		X						
3		X		X				
4		X		X	X			
5		X		X	X	X		
6		X		X			X	X
7	X	X	X	X			X	X
8		X		X			X	

*Configuration composed of basic F-4C model with addition of components indicated in line across table.

Table 2. Loads Due to Pylon.

S_{MF}; $M_\infty = 0.6$

(a) $\alpha_s = 0°$ $Z_p/D = 0$

	Z_p/D	ΔCN	ΔCY	ΔCLM	ΔCLN	ΔCLL
Data	0.07	0.063	-.019	-.206	0.028	0.002
Theory	0	.031	-.010	-.145	.001	0

(b) $\alpha_s = 0°$ $Z_p/D = 1.0$

Data	1.20	0.030	-.008	-.100	0.012	0.001
Theory	1.00	.016	-.004	-.077	.001	0

(c) $\alpha_s = 4°$ $Z_p/D = 0$

Data	0.10	0.069	-.061	-.220	0.071	0
Theory	0	.028	-.048	-.138	.051	0.001

(d) $\alpha_s = 4°$ $Z_p/D = 1.0$

Data	1.24	0.031	-.024	-.096	0.031	-.003
Theory	1.00	.020	-.022	-.072	.029	0

Table 3. Loads Due to Rack.

S_{MF}; $M_\infty = 0.6$

(a) $\alpha_s = 0°$ $Z_p/D = 0$

	Z_p/D	ΔCN	ΔCY	ΔCLM	ΔCLN	ΔCLL
Data	0.07	0.116	-.059	-.222	-.003	0.007
Theory	0	.051	.001	-.035	-.002	0

(b) $\alpha_s = 0°$ $Z_p/D = 1.0$

Data	1.21	0.037	-.015	-.086	0.045	0.001
Theory	1.00	.024	.001	-.027	-.001	0

(c) $\alpha_s = 4°$ $Z_p/D = 0$

Data	0.07	0.042	-.196	0	-.034	+.039
Theory	0	.050	+.001	0.031	-.001	0

(d) $\alpha_s = 4°$ $Z_p/D = 1.0$

Data	1.23	0.019	-.043	-.063	0.040	0
Theory	1.00	.024	0	-.024	0	0

Table 4. Loads Due to Shoulder Stores.

S_{MF}; $M_\infty = 0.6$

(a) $\alpha_s = 0°$ $Z_p/D = 0$

	Z_p/D	CN	CY	CLM	CLN	CLL
Data	0.07	0.456	-.018	-1.049	-.049	0.006
Theory	0	.334	.008	-.605	-0.012	0

(b) $\alpha_s = 0°$ $Z_p/D = 1.0$

Data	1.2	0.201	-.008	-.452	-.021	0.003
Theory	1.0	.190	.003	-.380	-.010	0

(c) $\alpha_s = 4°$ $Z_p/D = 0$

Data	0.07	0.237	-.063	-.955	-.022	0.208
Theory	0	.320	.006	-.551	-.008	-.005

(d) $\alpha_s = 4°$ $Z_p/D = 1.0$

Data	1.23	0.130	0	-.389	-.070	0.013
Theory	1.0	.181	0.005	-.385	-.007	0

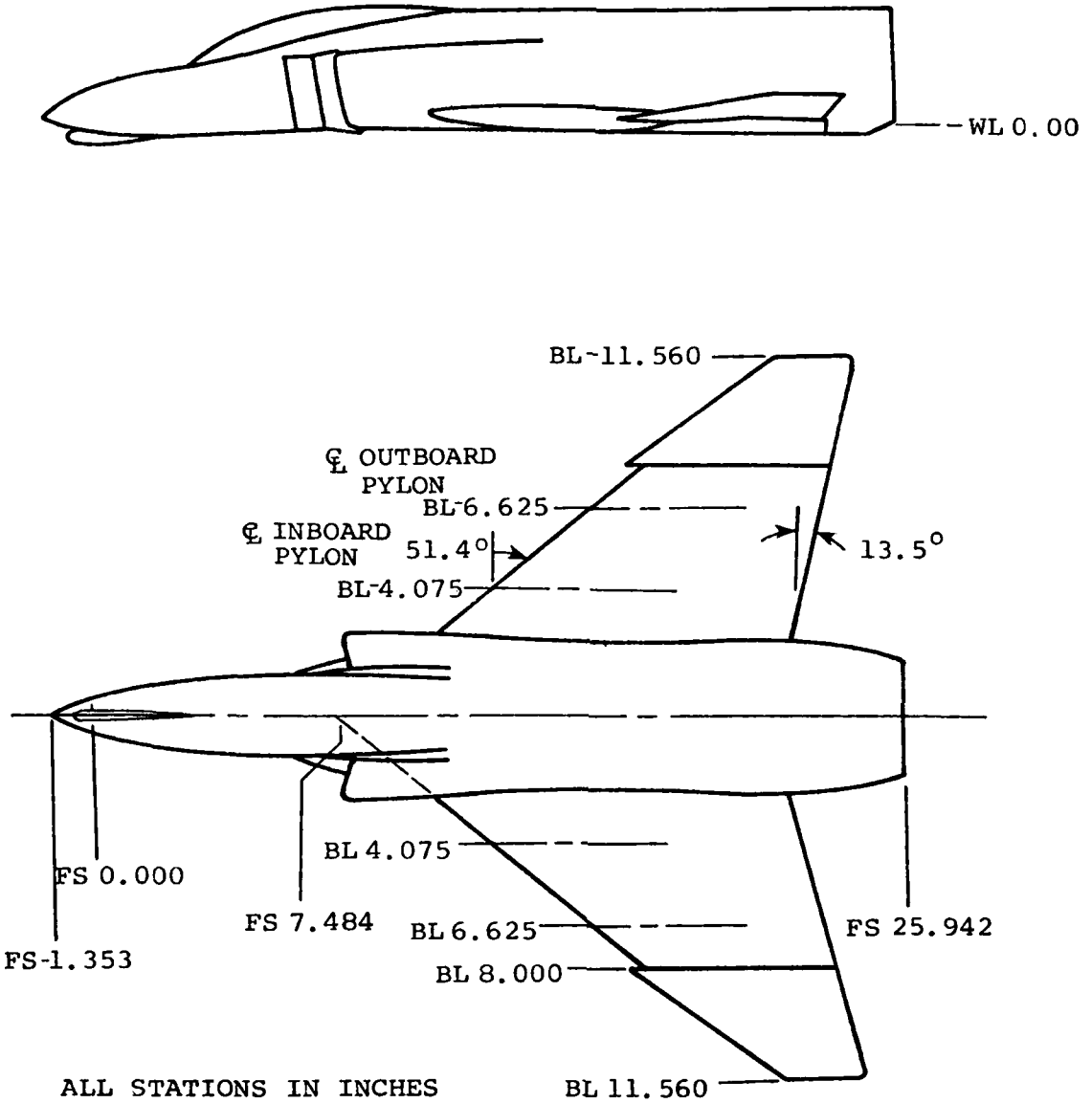

Figure 1. Five-Percent Scale Model of the F-4C Aircraft.

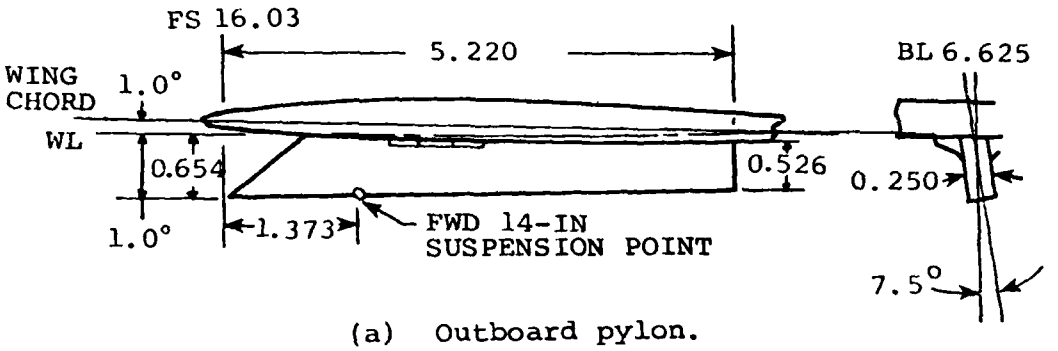

(a) Outboard pylon.

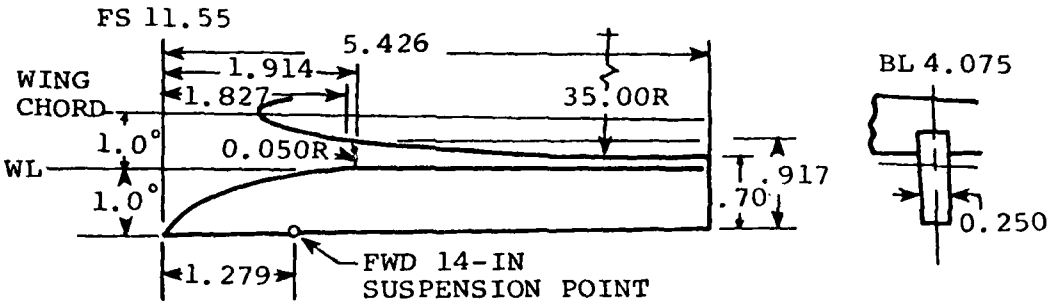

(b) Inboard pylon.

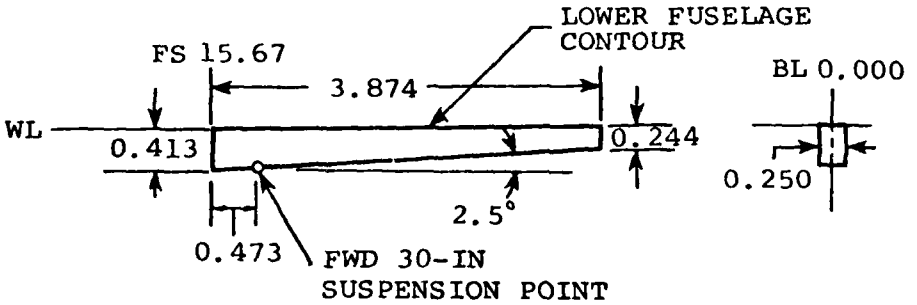

ALL DIMENSIONS IN INCHES

(c) Center pylon.

Figure 2. Details of the Models of the F-4C Pylons.

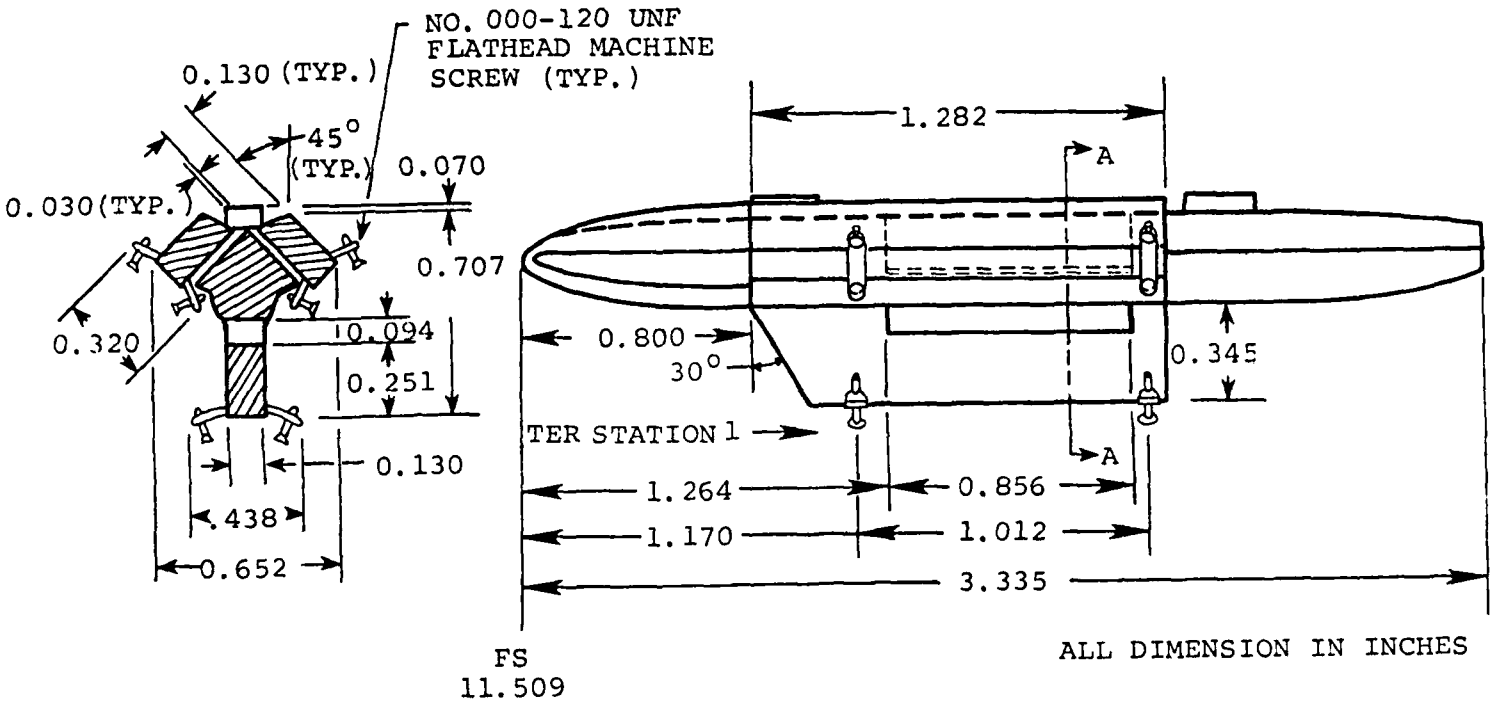

Figure 3. Details of the Model of the Triple Ejector Rack.

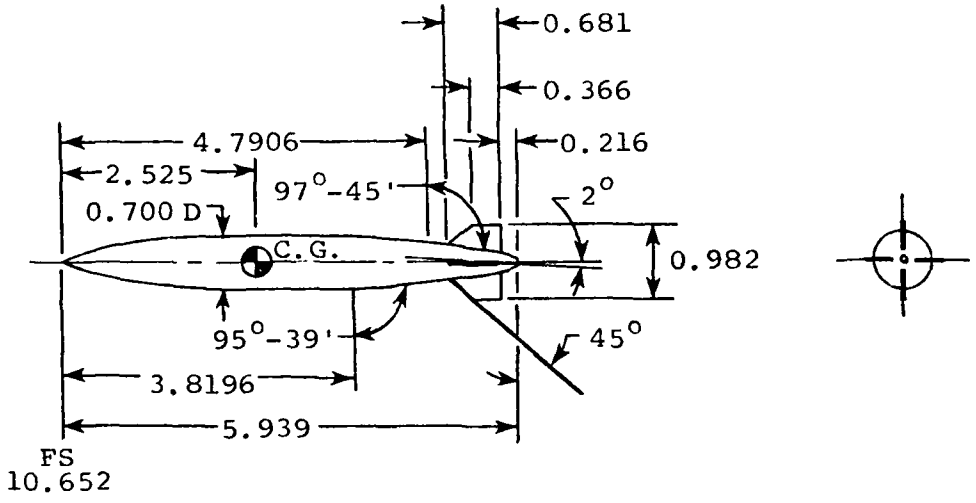

(a) Actual configuration, store S_{AF}.

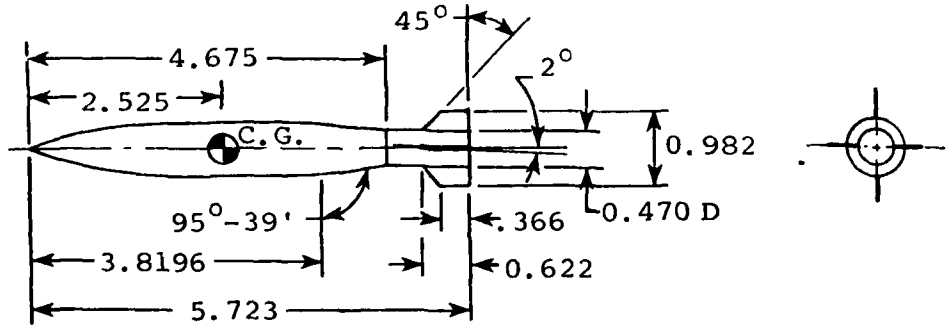

ALL DIMENSIONS IN INCHES

(b) Configuration modified for sting support, store S_{MF}.

Figure 4. MK-83 Bomb Models.

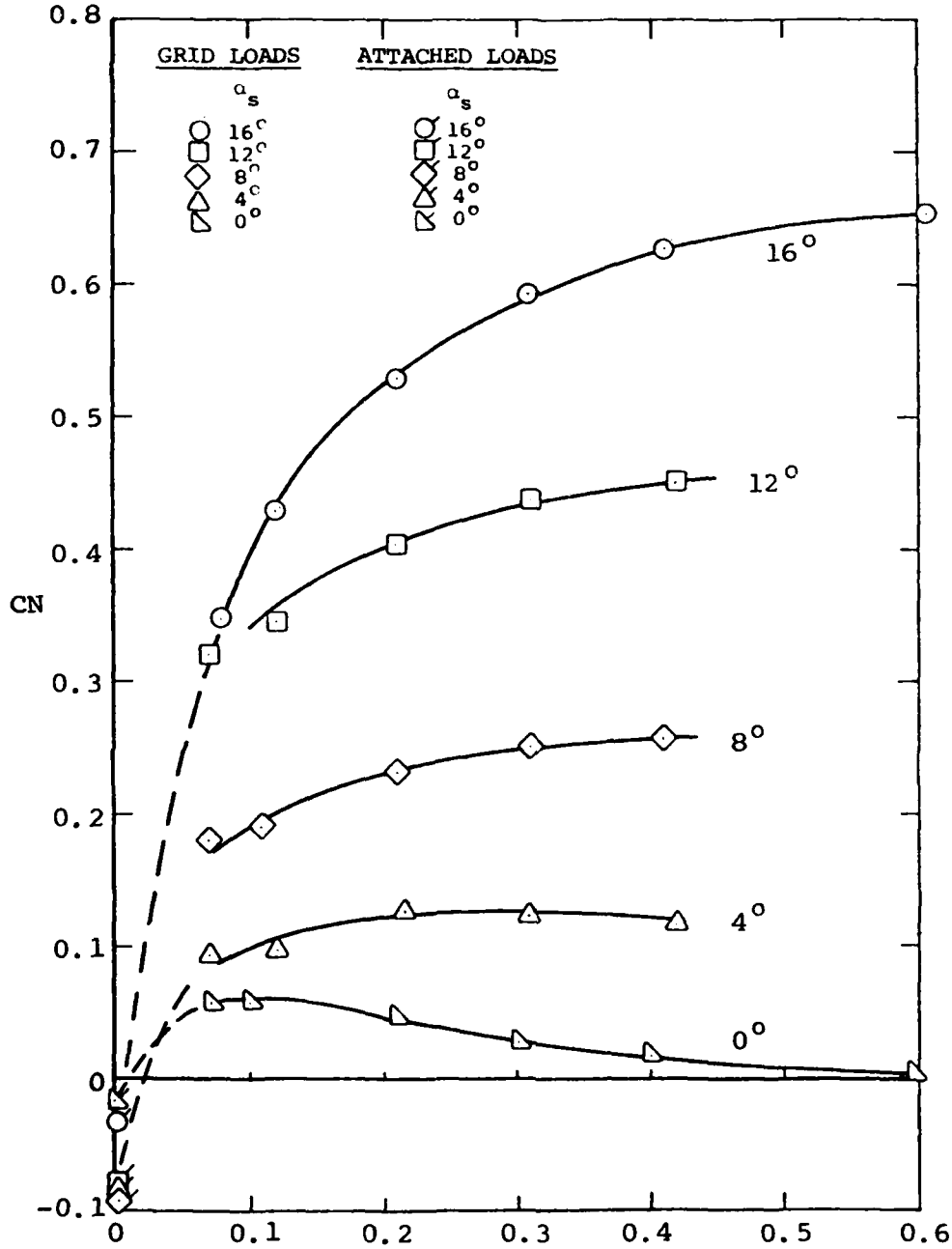

(a) Normal-force coefficient.

Figure 5. Comparison of Attached and Grid Loads for Store S_{MF} in Combination with Configuration 3 at M_∞ = 0.6.

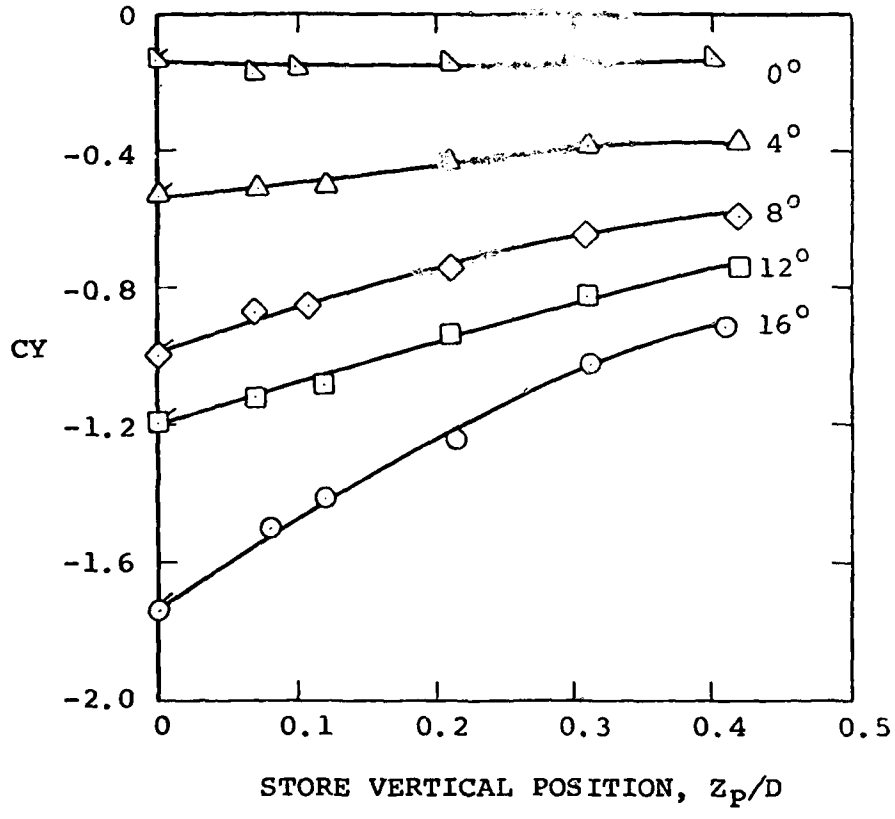

(b) Side-force coefficient.

Figure 5. Continued

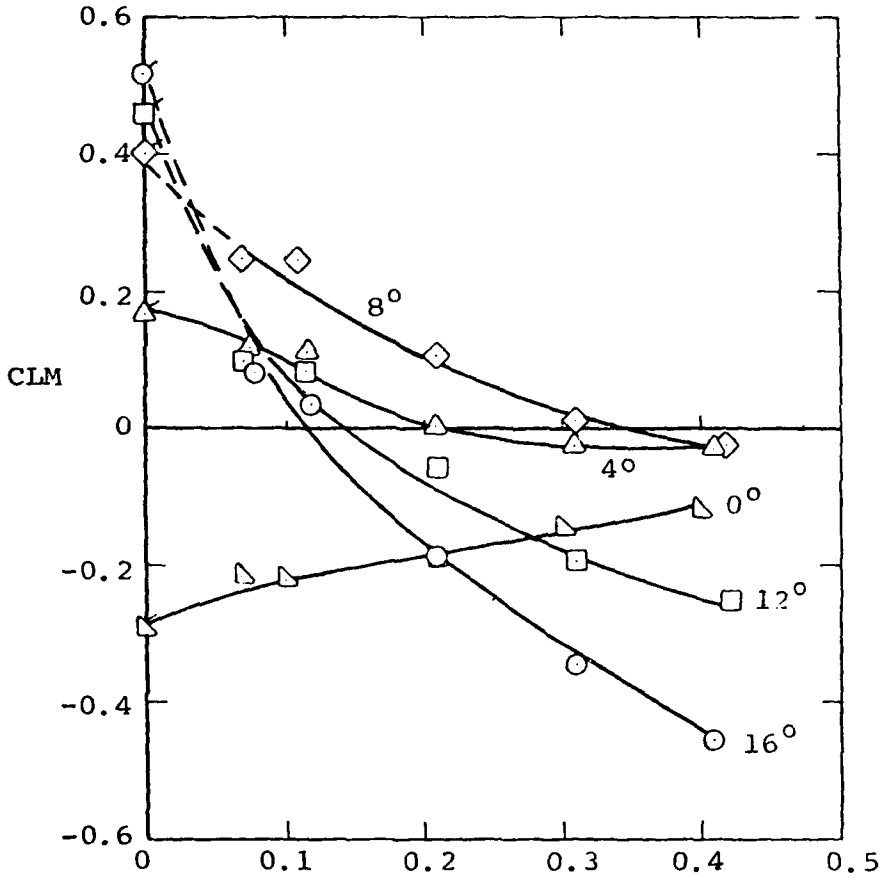

(c) Pitching-moment coefficient.

Figure 5. Continued

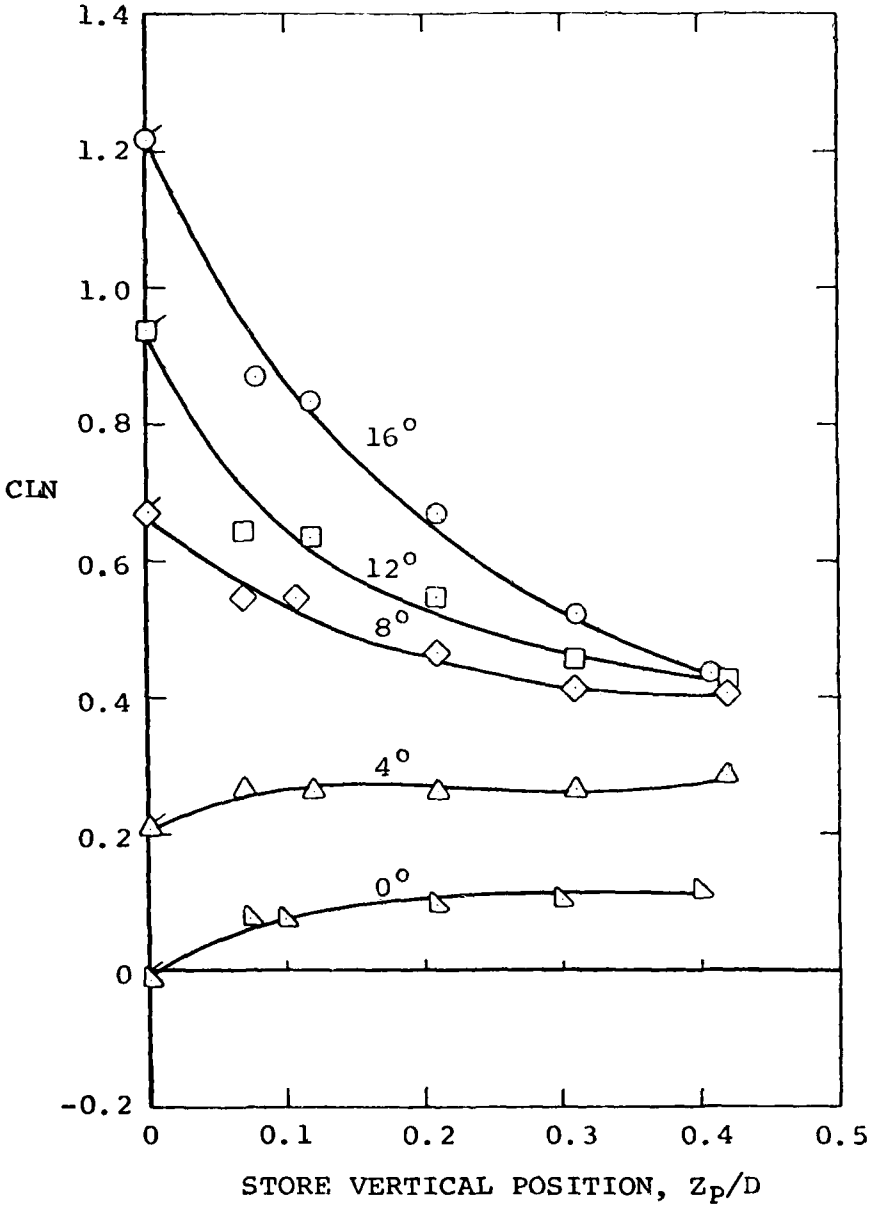

(d) Yawing-moment coefficient.

Figure 5. Continued

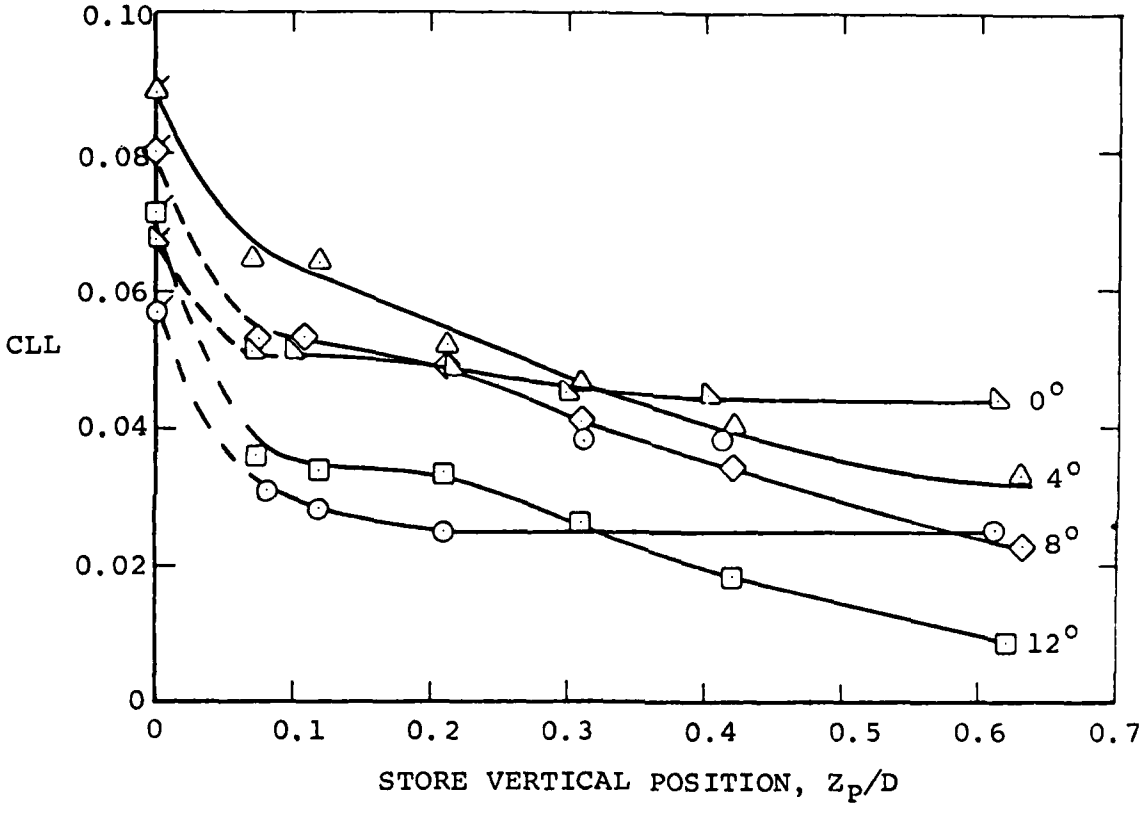

(e) Rolling-moment coefficient.

Figure 5. Concluded

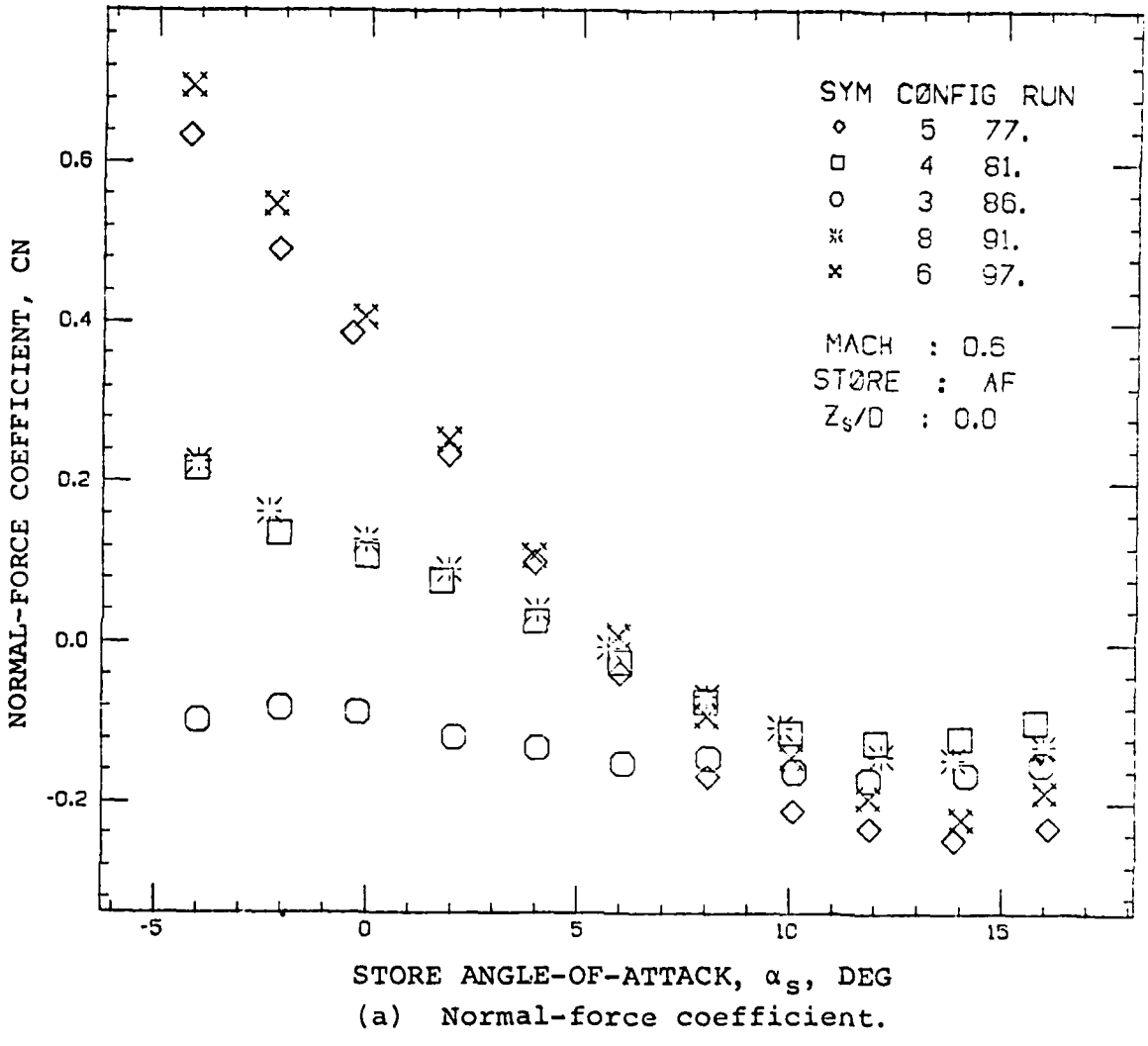

(a) Normal-force coefficient.

Figure 6. Effect of Airplane Configuration on Attached Loads of Bottom Store S_{AF} at M_∞ = 0.6.

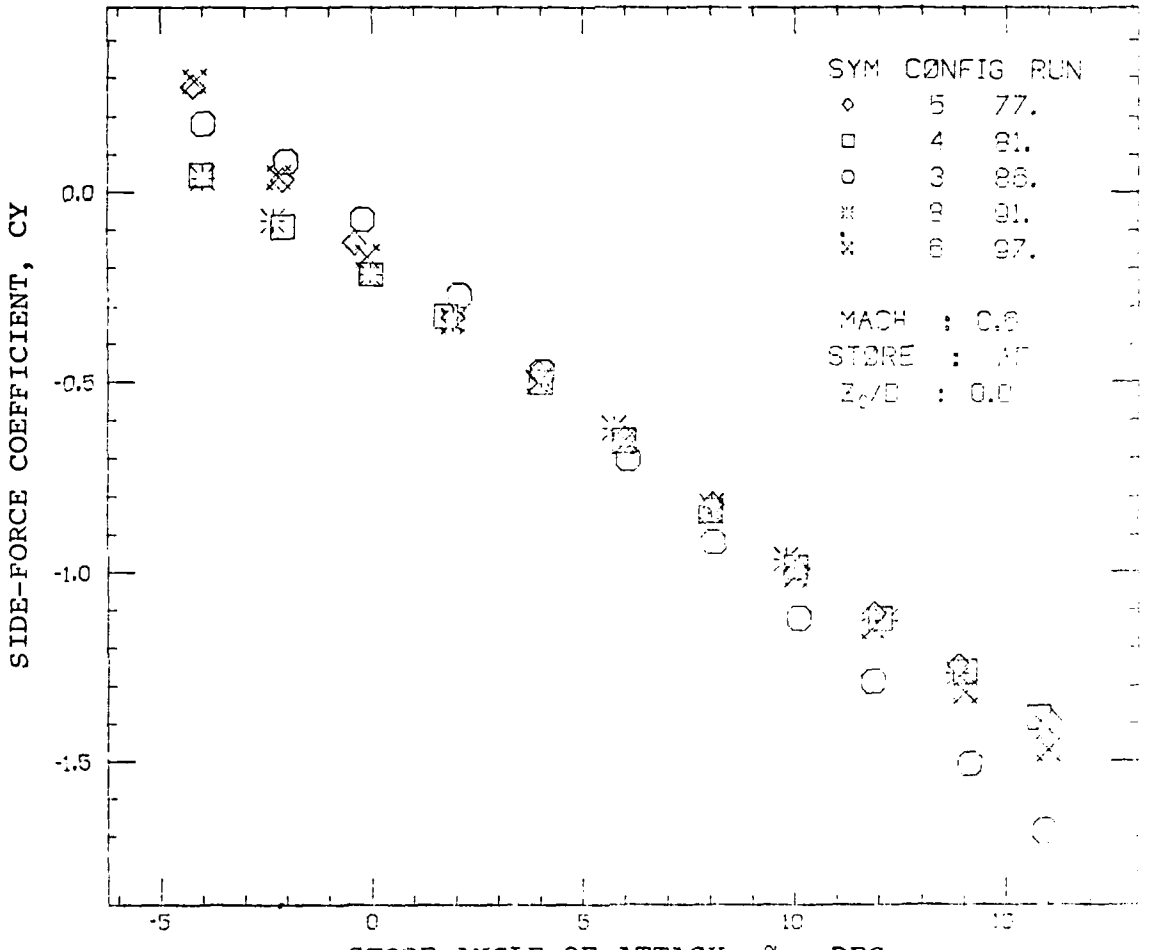

(b) Side-force coefficient.

Figure 6. Continued

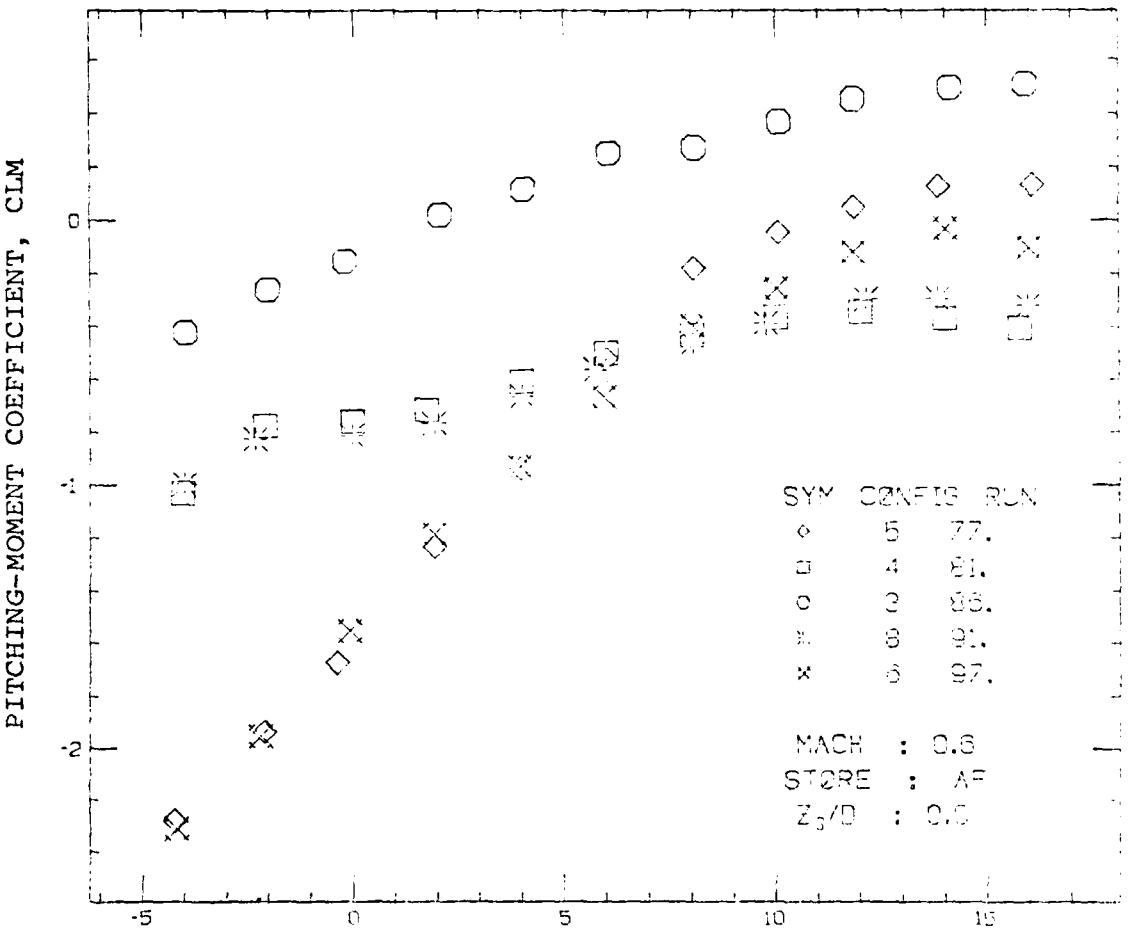

STORE ANGLE-OF-ATTACK, α_s, DEG

(c) Pitching-moment coefficient.

Figure 6. Continued

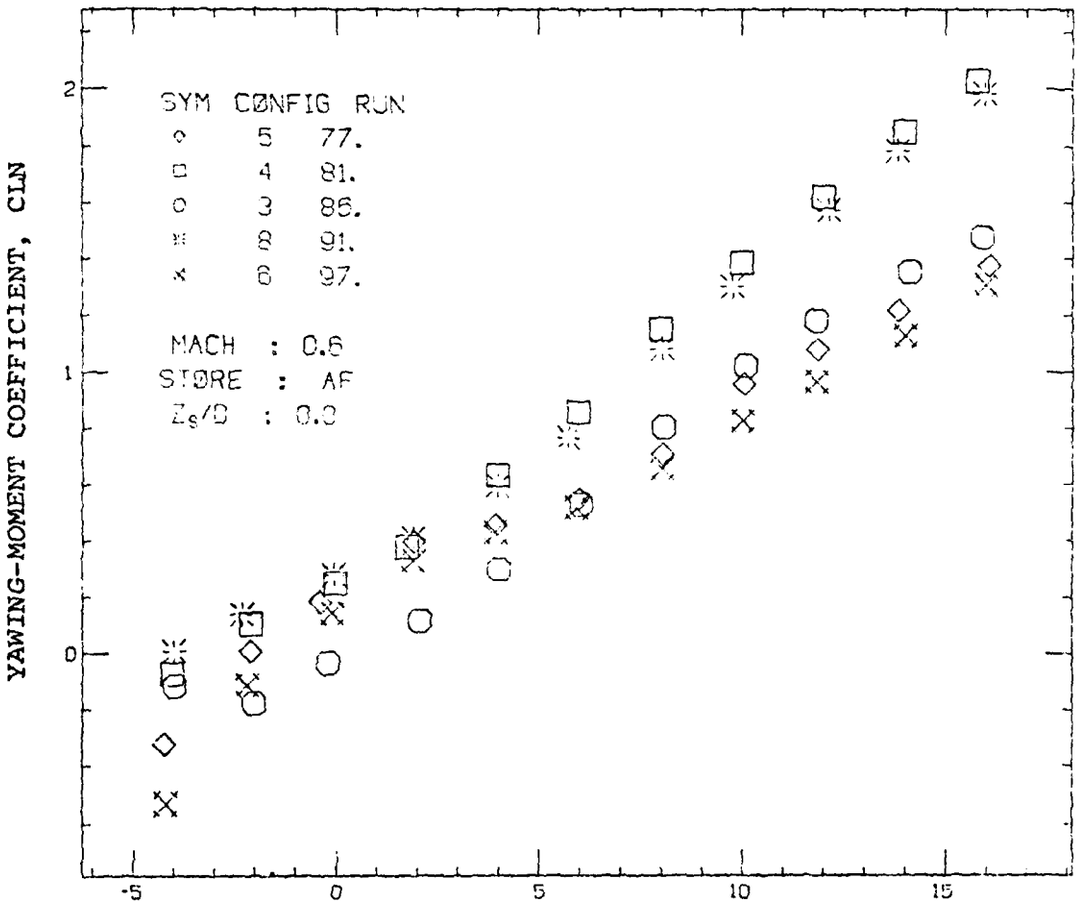

(d) Yawing-moment coefficient.

Figure 6. Continued

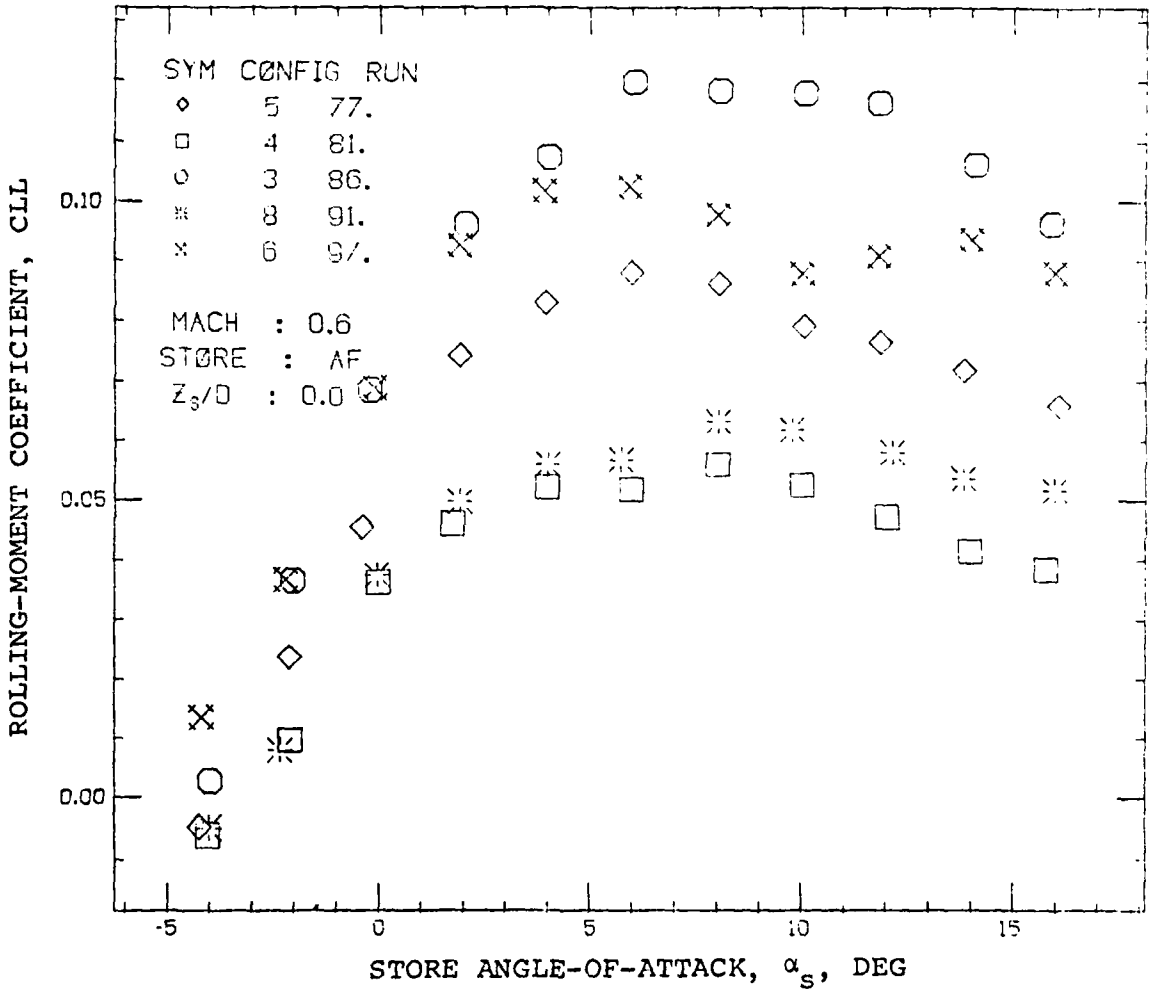

(e) Rolling-moment coefficient.

Figure 6. Concluded

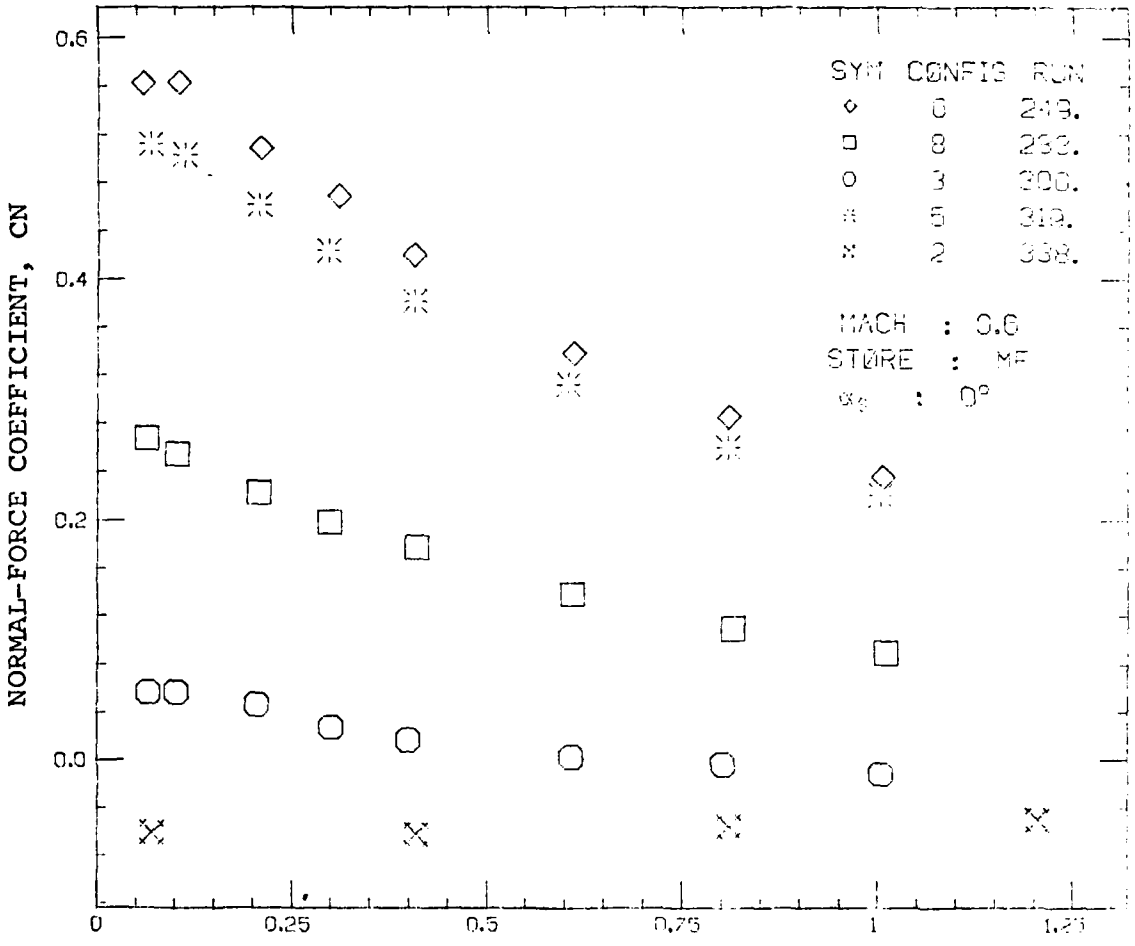

(a) Normal-force coefficient.

Figure 7. Grid Loads on Store S_{MF} as Influenced by Airplane Configuration; $M_\infty = 0.6$, $\alpha_s = 0°$.

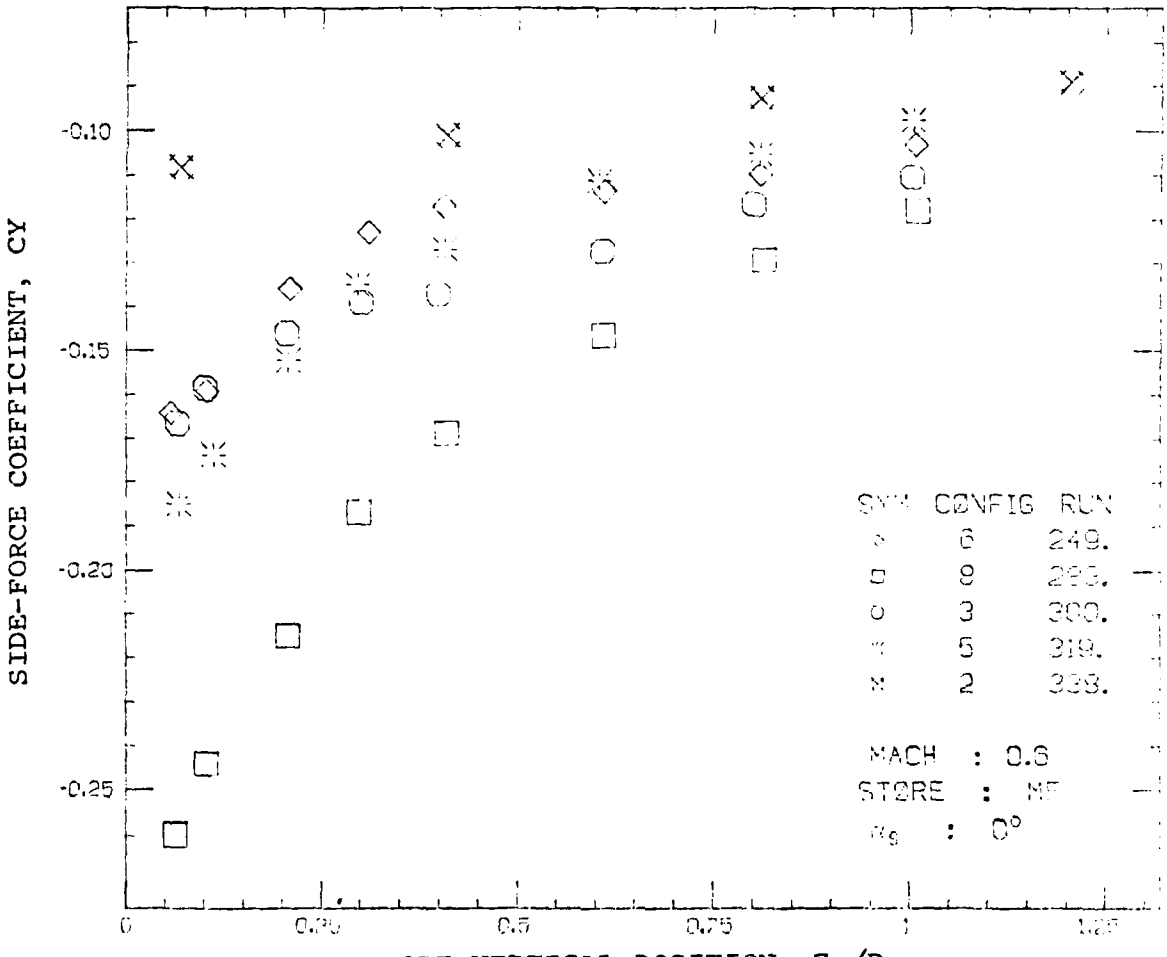

(b) Side-force coefficient.

Figure 7. Continued

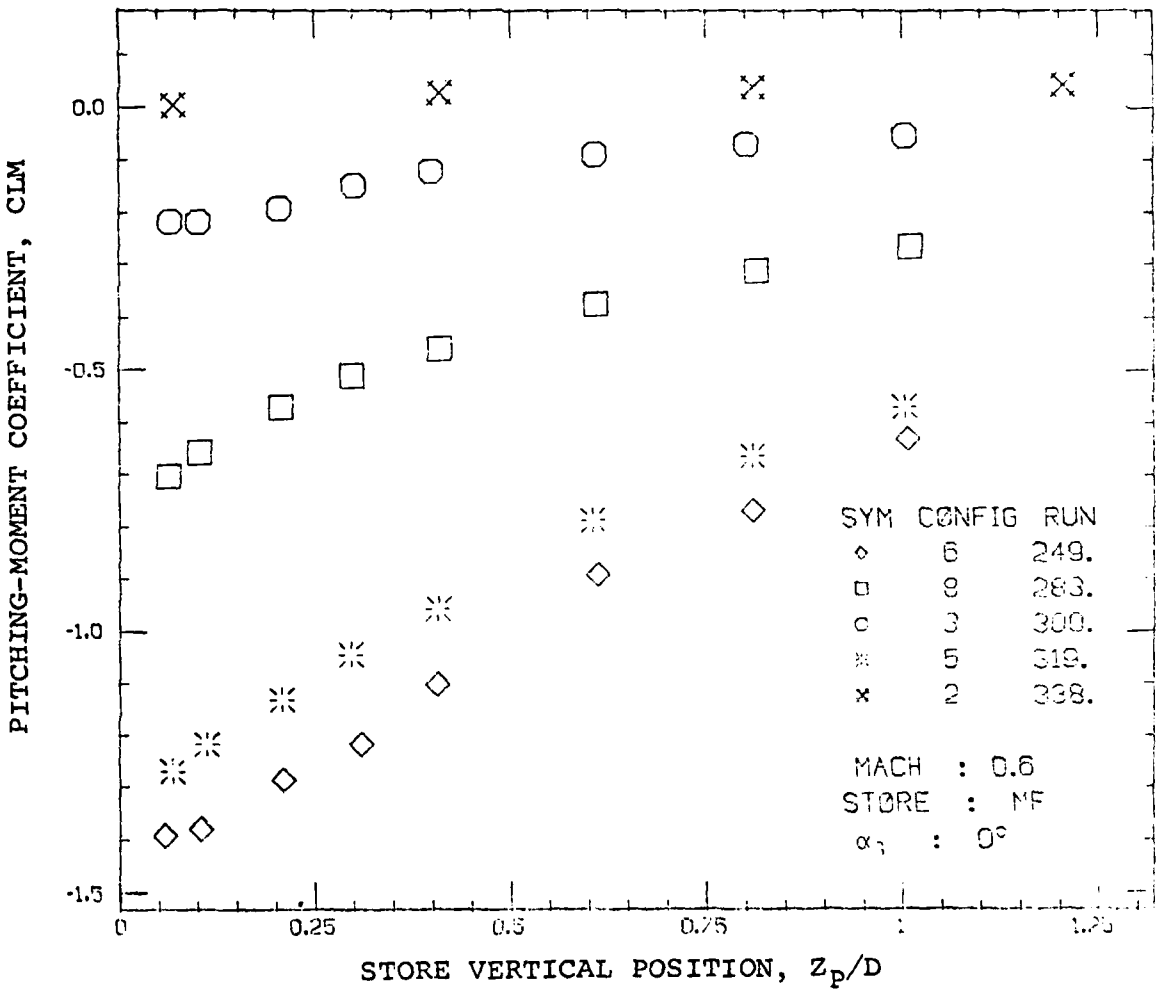

(c) Pitching-moment coefficient.

Figure 7. Continued.

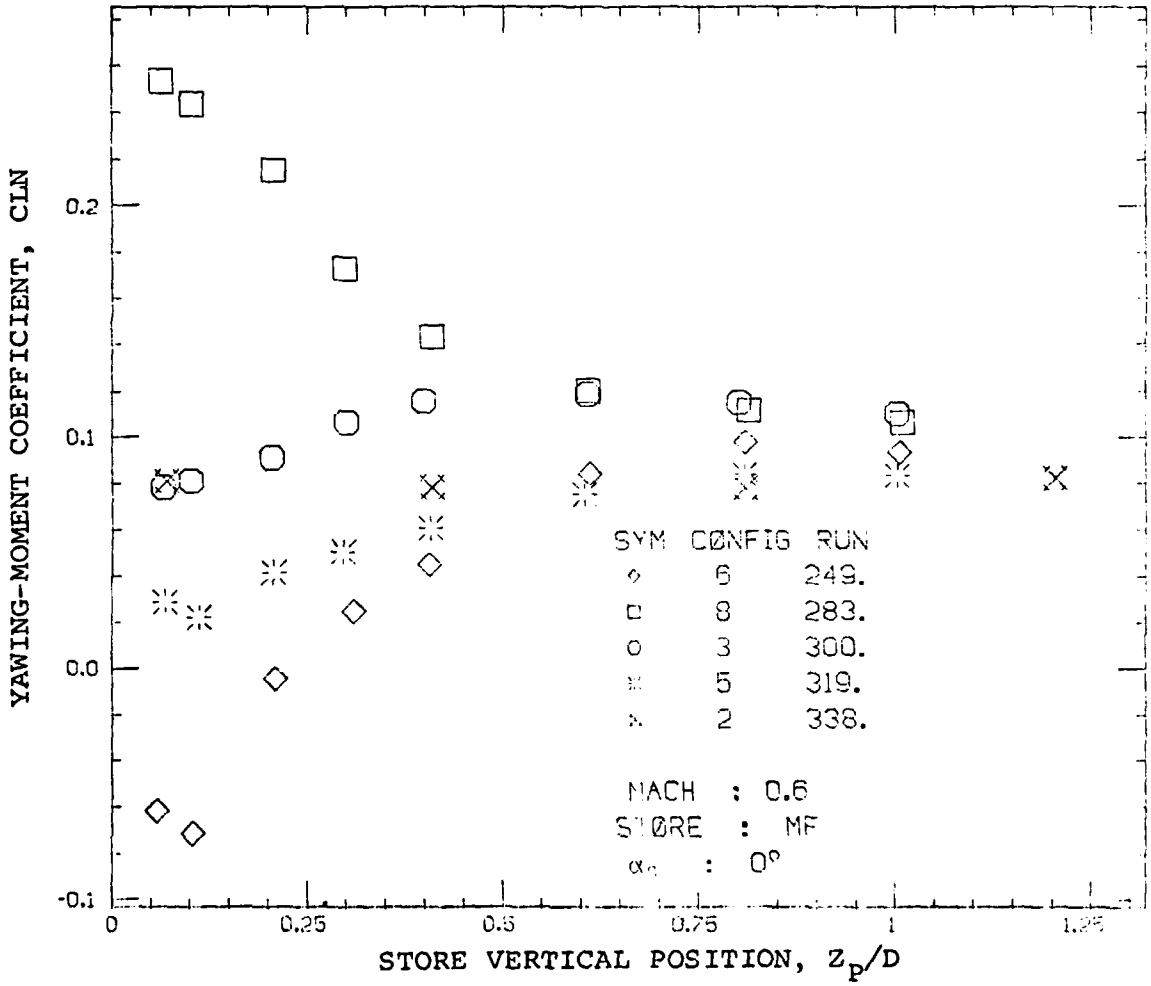

(d) Yawing-moment coefficient.

Figure 7. Continued.

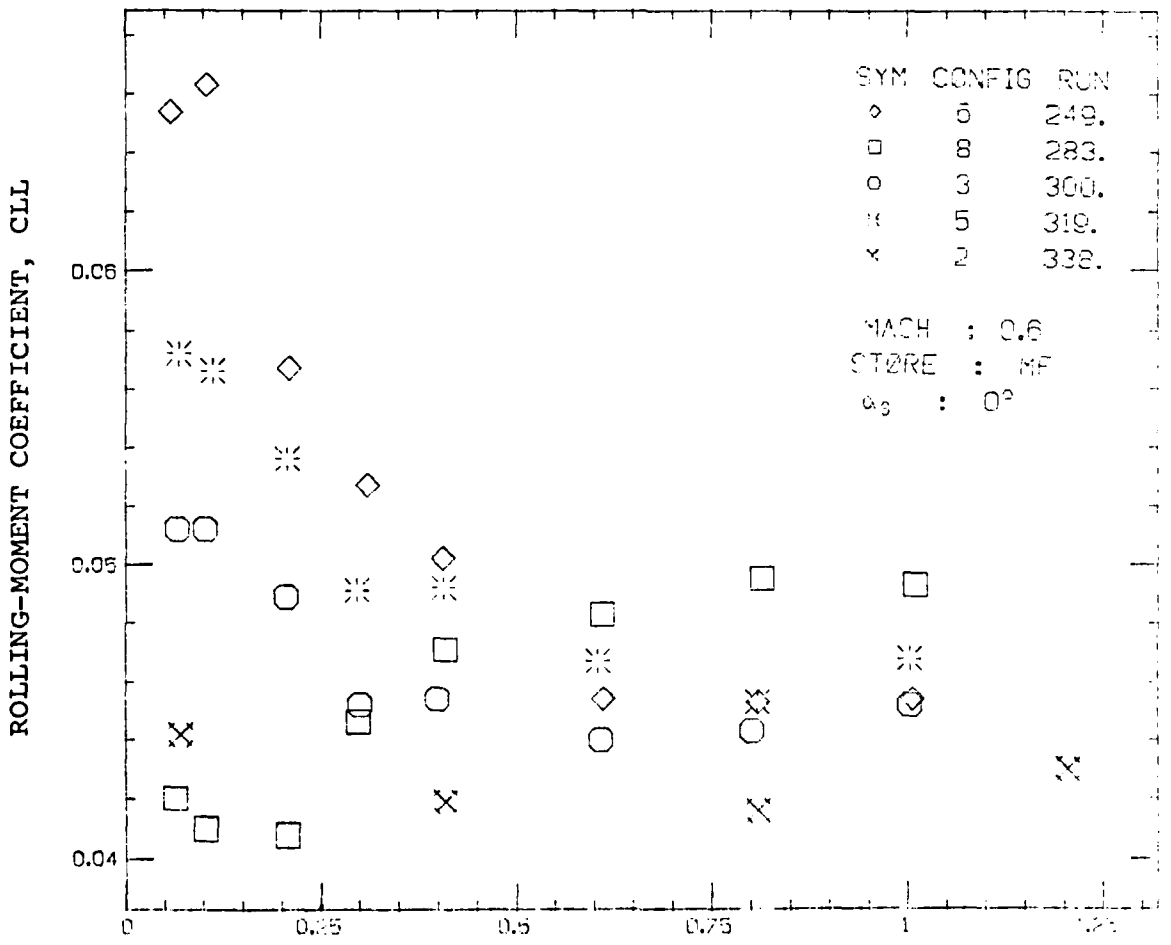

(e) Rolling-moment coefficient.

Figure 7. Concluded

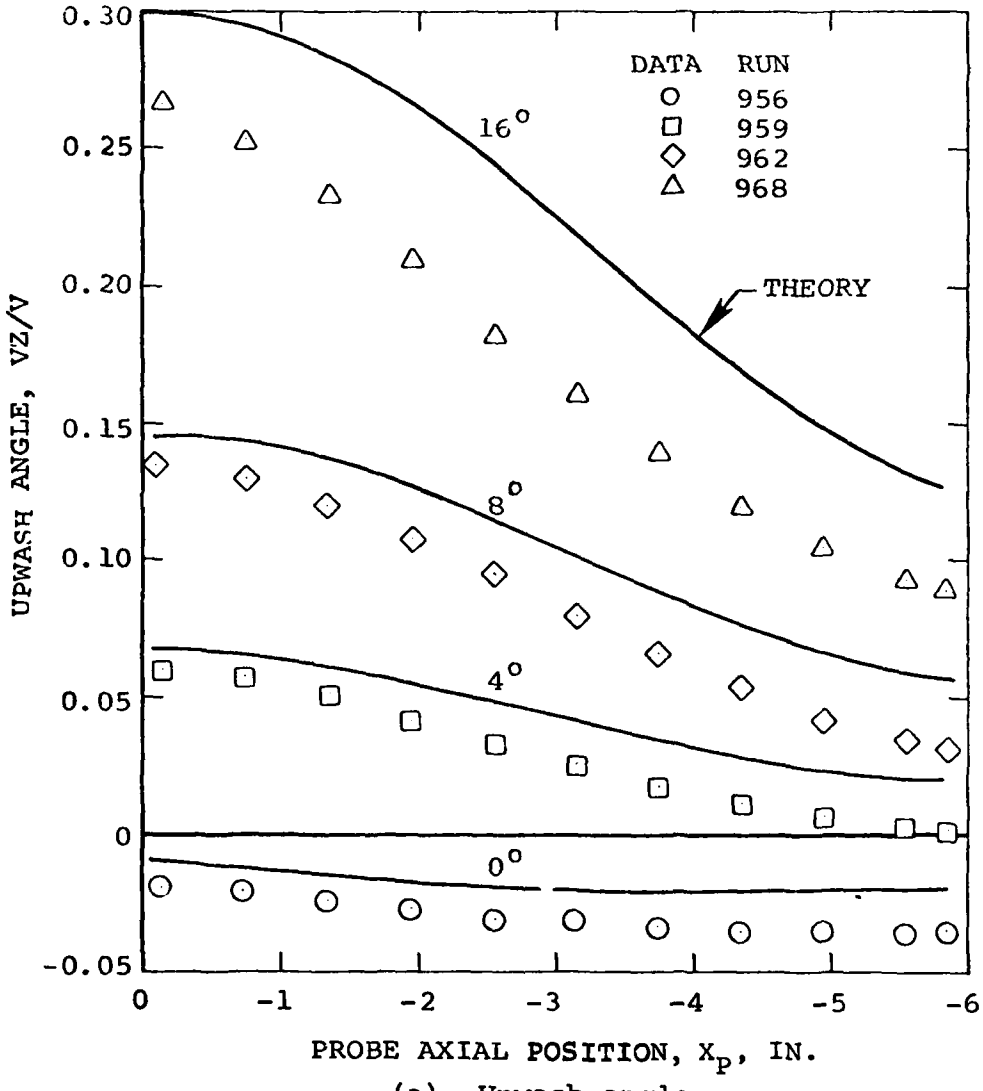

(a) Upwash angle.

Figure 8. Flow Field Comparisons for Clean Airplane at $M_\infty = 0.6$ and $Z_p/D = 0$ as a Function of Angle of Attack.

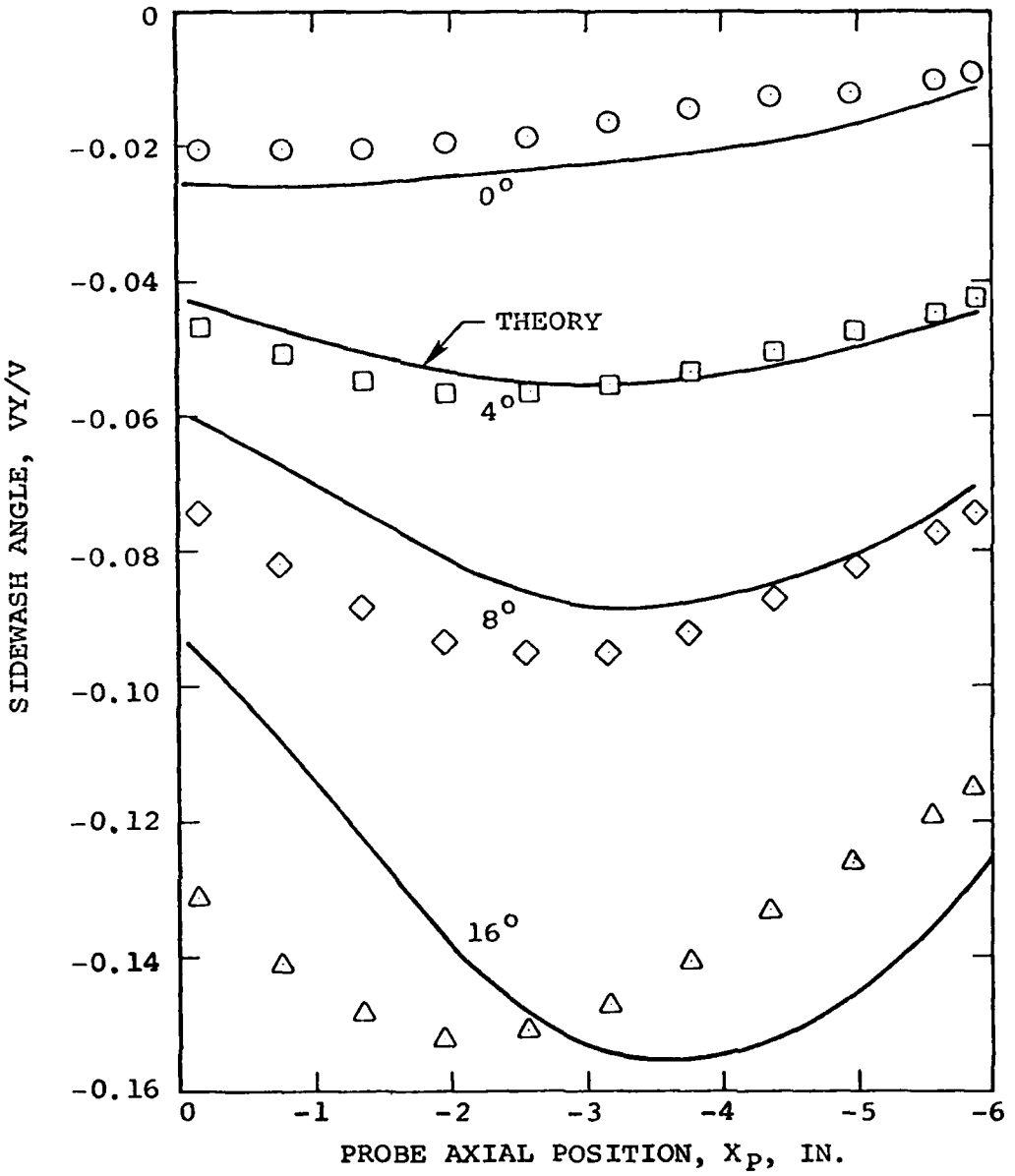

(b) Sidewash angle.

Figure 8. Concluded

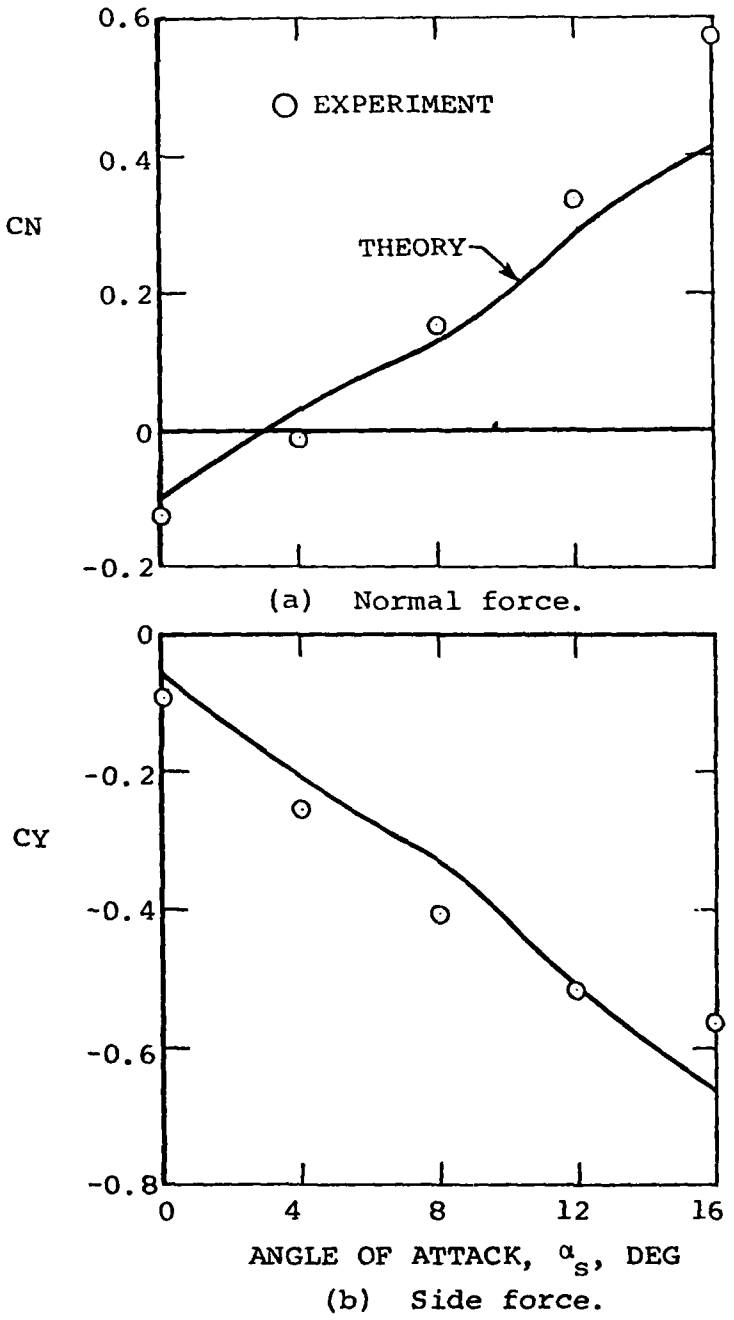

Figure 9. Loads on Store S_{MF} in Combination with Clean Airplane at $M_\infty = 0.6$, $Z_p/D = 0$.

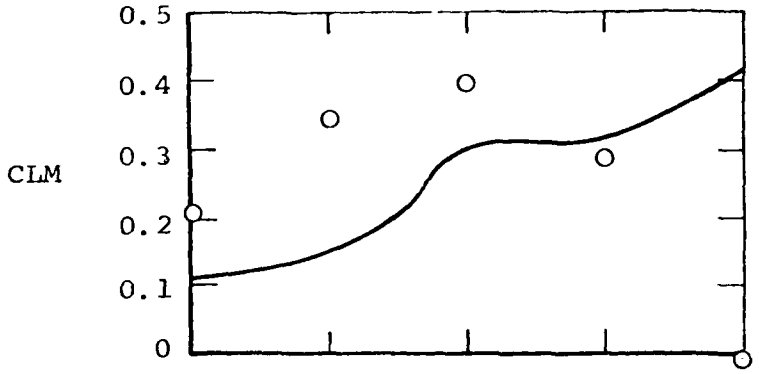

(c) Pitching moment.

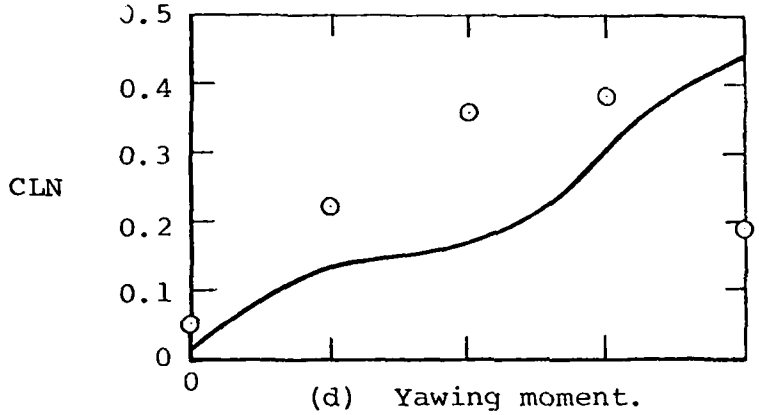

(d) Yawing moment.

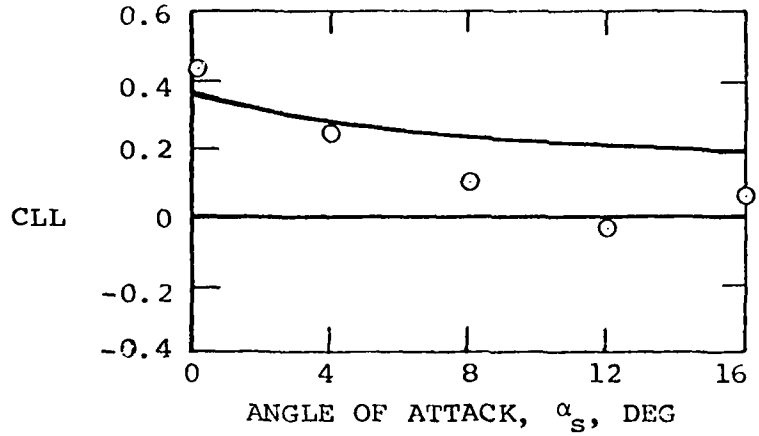

(e) Rolling moment.

Figure 9. Concluded

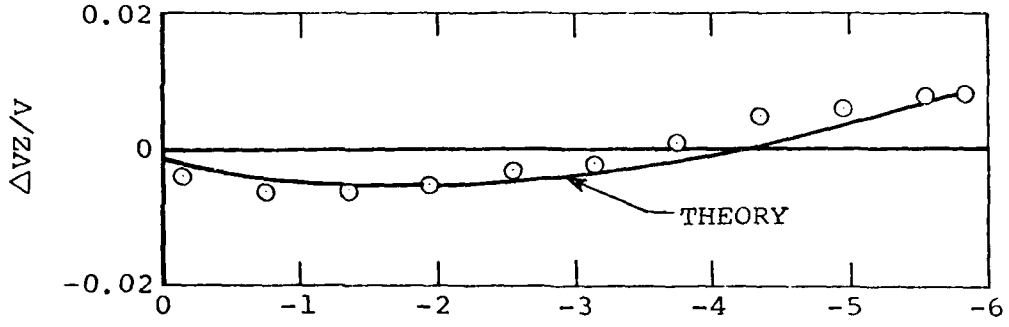

(a) Upwash angle.

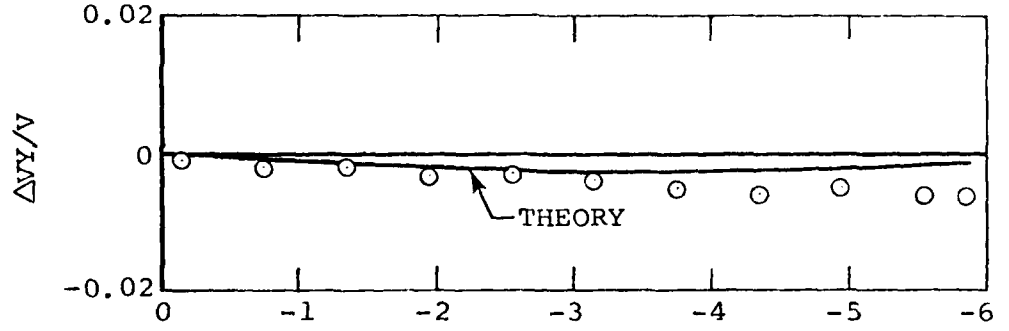

(b) Sidewash angle.

Figure 10. Effect of Adding a Pylon to the Clean Airplane on the Flow Angles Along the Centerline Position of the Bottom Store at $M_\infty = 0.6$; $\alpha_s = 0°$; $Z_p/D = 0$.

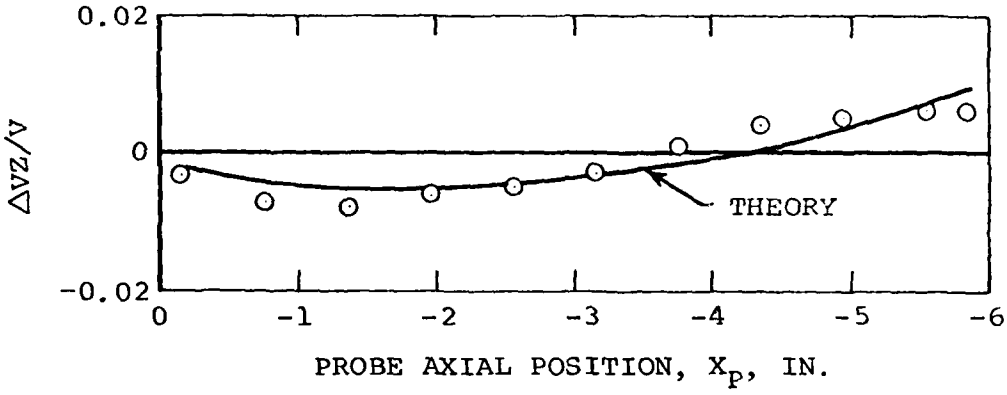

(a) Upwash angle.

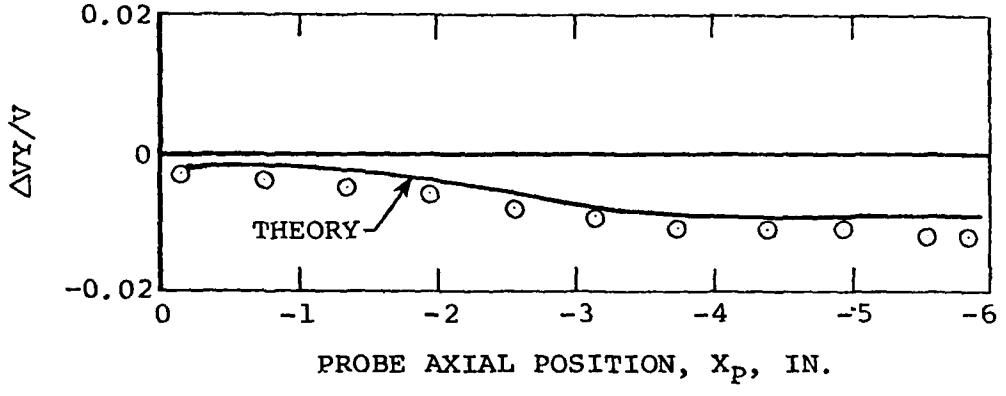

(b) Sidewash angle.

Figure 11. Effect of Adding a Pylon to the Clean Airplane on the Flow Angles Along the Centerline Position of the Bottom Store at $M_\infty = 0.6$; $\alpha_s = 4°$; $Z_p/D = 0$.

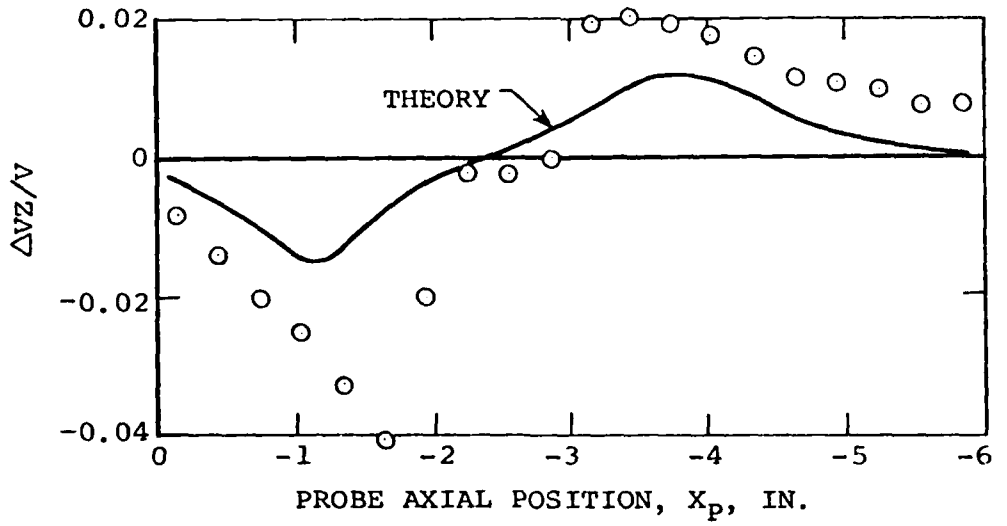

(a) Upwash angle.

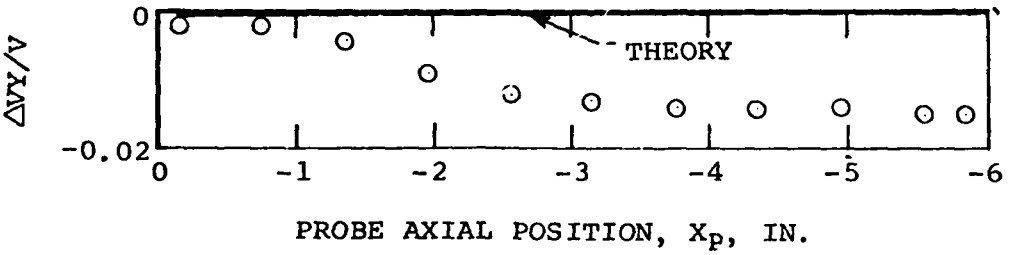

(b) Sidewash angle.

Figure 12. Effect of Adding TER to Pylon on the Flow Angles Along the Centerline Position of the Bottom Store at $M_\infty = 0.6$; $\alpha_s = 0°$; $Z_p/D = 0$.

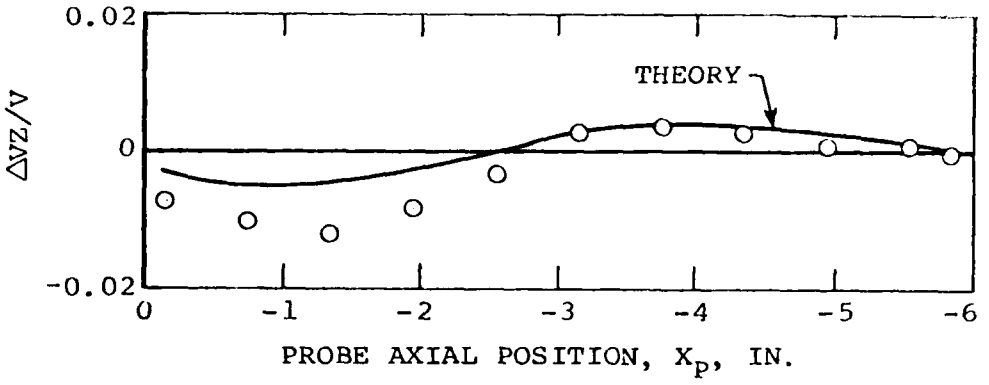

(a) Upwash angle.

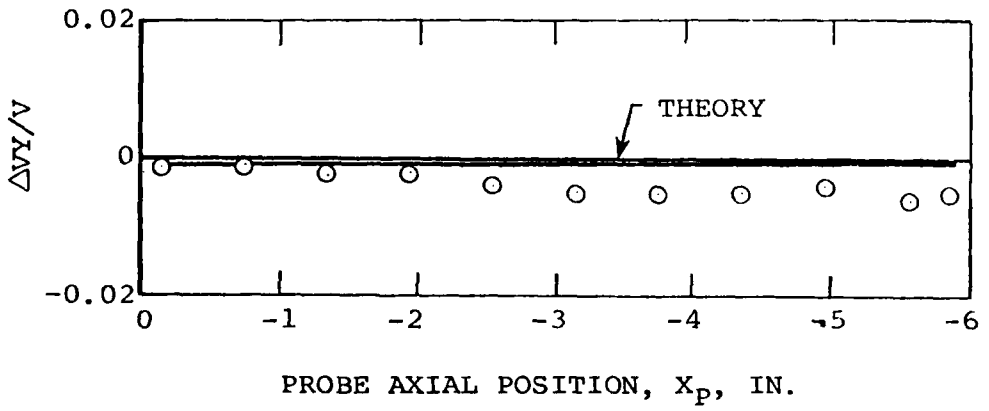

(b) Sidewash angle.

Figure 13. Effect of Adding TER to Pylon on the Flow Angles Along the Centerline Position of the Bottom Store at $M_\infty = 0.6$; $\alpha_s = 0°$; $Z_p/D = 1.0$.

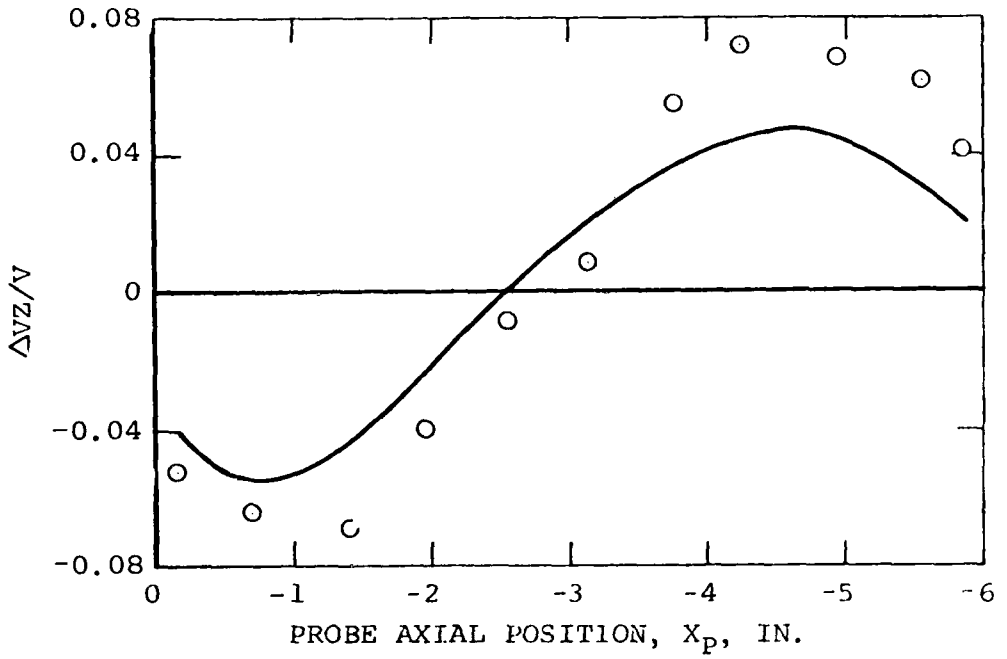

(a) Upwash angle.

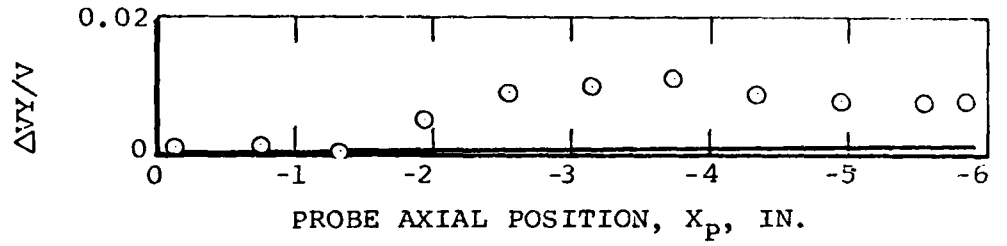

(b) Sidewash angle.

Figure 14. Effect of Adding Shoulder Stores to Configuration 3 on the Flow Angles Along the Centerline Position of the Bottom Store; $M_\infty = 0.6$, $\alpha_s = 0°$, $Z_p/D = 0$.

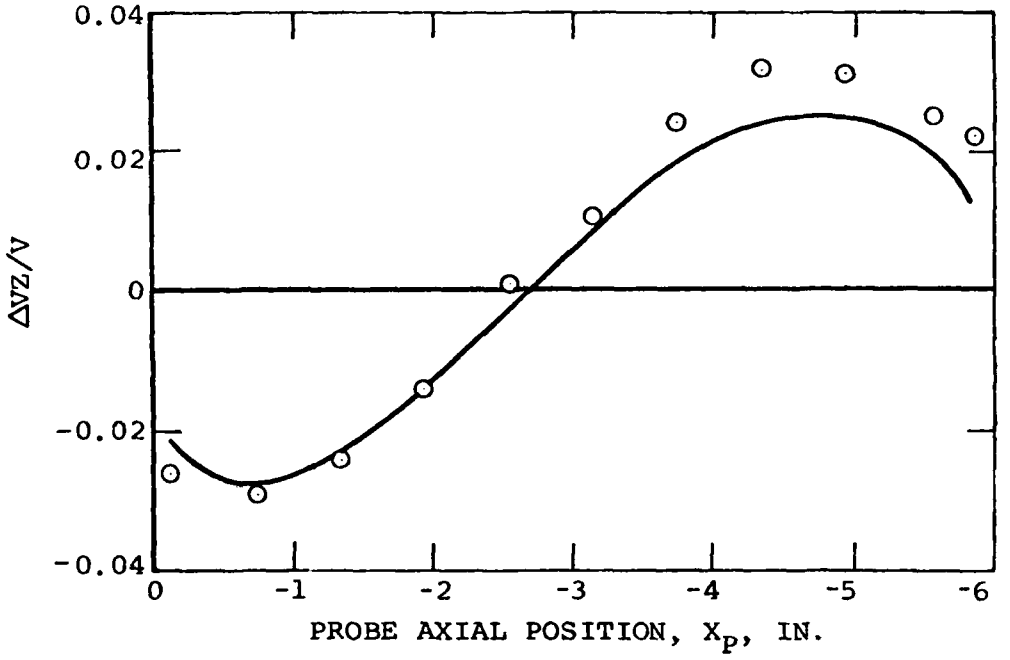

(a) Upwash angle.

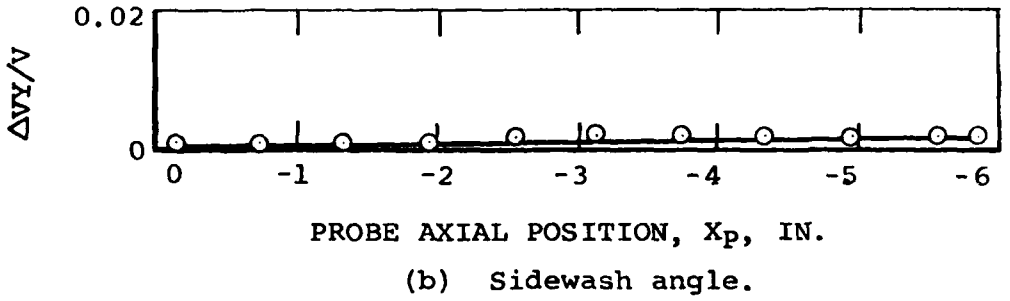

(b) Sidewash angle.

Figure 15. Effect of Adding Shoulder Stores to Configuration 3 on the Flow Angles Along the Centerline Position of the Bottom Store; $M_\infty = 0.6$, $\alpha_s = 0°$, $Z_p/D = 1.0$.


NI
DATE
ILME